

# **Fireball Physics and Determination of Meteorite Fall Locations**

Frank Sanders, DMNS/DESS Research Associate  
for The Denver Museum of Nature and Science Meteorite Workshop  
Department of Earth and Space Sciences: Geology

23 July 2000

## FOREWORD AND ACKNOWLEDGMENT

In November 1995 an exceptionally bright fireball streaked across Colorado skies, travelling roughly southeast from the vicinity of Pikes Peak to the plains of rural Crowley County. The visible event and associated acoustics were reported from locations across much of the state. The Curator of Geology at the Denver Museum of Natural History (DMNH), Jack Murphy, initiated an investigation to determine the fireball flight path and the probable location of the resulting fall, if any existed. The author, initially involved by Murphy in the flight path study, became intrigued by the physics of fireballs, and specifically in determining answers to the following questions:

- Why do fireballs occur? Why and how do fireballs differ from ordinary meteors?
- Do fireballs usually result in meteorite falls?
- How can fireball flight paths be accurately and efficiently determined?
- If falls occur, can the most probable fall locations be determined from fireball flight path data?
- If the answer to the item above is yes, then what is the relationship? Can it be modelled analytically or numerically, and if so, how? Can original meteoroid orbits also be accurately determined?

Subsequent to the 1995 fireball investigation, and as a development of those activities, Jack Murphy initiated a series of meteorite workshops at DMNH. Participants were volunteers who had already completed the Department of Earth Sciences (now the Department of Earth and Space Sciences (DESS)) paleontology certification program. These persons were known to be capable of dedicatedly approaching the problems associated with collecting and analyzing fireball data from eyewitness accounts.

The author was privileged to assist Jack in the development of these workshops. He pursued answers to the questions posed above as the workshop series progressed, and as additional Colorado fireballs were investigated during the following years.

In this paper, the author is now able to report answers to the questions posed above. The answers have depended upon the creation by the author of two physical models: one for fireball flight physics, and the other for free-fall of a high-velocity projectile from a high altitude to the earth's surface, modified by atmospheric resistance. The first model is generated and solved analytically, while the second is solved by numerical integration. Taken together, the two models explain the how and why of fireballs, and predict the locations where meteorite falls should be found subsequent to fireball events.

As a corollary, the author explains the geometry necessary to locate meteorite falls from eyewitness accounts and how (hopefully, for future fireball events) all-sky camera data will be used to localize fireball velocities (direction and speed) to high precision. A hypothetical sky camera network is described, and the processing of resulting data is described so as to yield not only probable fall locations but also the orbits from which the meteoroids that generate fireballs originate.

The author wishes to express his deepest gratitude to Jack Murphy for his inspiration and support in this entire effort. Without him, this effort would never have started, much less come to fruition. Jack Murphy's efforts represent the best of genuine scientific endeavor--an interesting problem formulated from common but underappreciated observations, and solved without funding, but with the application of sheer brain-power and persistence.

Frank Sanders  
10 March 2000

# Fireball Physics and Determination of Meteorite Fall Locations

Frank Sanders, DMNS/DESS Research Associate

for The Denver Museum of Nature and Science Meteorite Workshop

Department of Earth and Space Sciences: Geology

23 July 2000

## 1.0 INTRODUCTION

Meteorites are pieces of rock and metal that formed at approximately the origin of the solar system, and that have been swept out of solar orbits to the earth's surface. Derived primarily from asteroids and possibly cometary nuclei, they are the nearest physical links to the proto-solar system nebula.<sup>1</sup> Some meteoritic materials apparently condensed simultaneously with, or slightly before, the terrestrial planets. The information recorded within the most primitive of these materials provides significant clues to physical conditions within the proto-solar cloud.<sup>2</sup>

It is barely possible that some meteorites contain an indication of extraterrestrial life within our solar system. A few meteorites have been ejected from the surfaces of Mars and the moon, and one martian meteorite (ALH84001) has provided a highly tentative case for the possible existence of life on Mars during that planet's early history.<sup>3</sup>

Meteorites provide us with samples that will cost hundreds of millions of dollars to acquire through sample-return missions to comets, the asteroid belt and Mars. As one planetary scientist said years ago of ALH84001, "The first sample was free, but the next one's going to cost us about 300 million dollars."<sup>4</sup>

Given the importance of collecting meteorites in lieu of (or as an augmentation to) expensive sample-return missions, it is surprising that more effort has not been expended on the problem of locating meteorite falls from observations of their visible precursor phenomena, called fireballs. In connection with a 1995-1998 series of fireball investigations and meteorite workshops at the

---

<sup>1</sup>Excellent summaries are presented in Stuart Ross Taylor, *Solar System Evolution: A New Perspective*, Cambridge University Press, Chapter 3, 1990; and Clark Chapman in *The New Solar System*, O'Leary and Chaikin, eds., Cambridge University Press, 1999.

<sup>2</sup> Ross, *ibid.*

<sup>3</sup>An excellent summary is presented in J. William Schopf, *The Cradle of Life: The Discovery of Earth's Earliest Fossils*, Chapter 12, Princeton University Press, 1999.

<sup>4</sup>Donald Goldsmith, *The Hunt for Life on Mars*, Penguin Books Ltd., New York, pg. 214.

Denver Museum of Nature and Science (DMNS),<sup>5</sup> the author undertook a survey of existing literature on the subject and found no systematic methodology for precisely connecting the location of a fall with information derived from observation of visible flight phenomena. The author therefore undertook a study of the physics of extraterrestrial material entering the earth's atmosphere.

This paper describes meteoroid atmospheric flight physics, and particularly the physics of fireball phenomena. Lacking quantitative sources on this subject, the author created a model of a meteoroid as a modified re-entry vehicle, and applied equations from technical literature related to re-entry vehicle physics and design, as referenced. On the final topic of determining likely strewnfield locations from observations of fireballs, the author's model and derivations are entirely original.

The mathematics and physics in this paper are written at the secondary school level, and may be used in future fireball workshops or in secondary schools as an adjunct to the author's proposed fireball camera network.

## 2.0 BACKGROUND: METEOROID ARRIVAL AT EARTH

It is necessary to first calculate the approximate speed at which a meteoroid may be expected to encounter the earth's upper atmosphere. This is performed in Problems 1-3, below.

### **Problem #1: Circular orbital speed**

- a) Derive the speed of a circular orbit for a small mass attracted by a much larger central body.
- b) Use this functional relationship to calculate the speed of the earth around the Sun.

#### **Solution:**

From dynamics, an inertial mass,  $m$ , rotating in circular motion at a radius,  $r_0$ , at a velocity,  $v$ , around a central point experiences a centripetal force:

$$F_{\text{inertial}} = \frac{mv_c^2}{r_0}$$

Newtonian gravitation postulates that every mass in the universe attracts every other mass in the universe with a gravitational force that is proportional (via the constant,  $G$ ) to the product of the two masses ( $m$  and  $M$ , in this case), and that is inversely proportional to the square of the distance,  $r_0$ , between the masses:

$$F_{\text{gravitational}} = \frac{GMm}{r_0^2}$$

---

<sup>5</sup>See Foreword and Acknowledgments. When the workshops began, the museum was called the Denver Museum of Natural History (DMNH).

In a circular orbit, the gravitational force and the centripetal force must be equal. Assuming that the equivalence principle<sup>6</sup> holds, the two equations are equated:

$$\frac{mv_c^2}{r_0} = \frac{GMm}{r_0^2}$$

and the quantity  $\frac{m}{r_0}$  is divided out of both sides to yield:

$$v_c^2 = \frac{GM}{r_0}$$

which implies that the velocity of a circular orbit is

$$v_c = \sqrt{\frac{GM}{r_0}}$$

For the velocity of the earth around the Sun, the values of the physical constants are:

$$G = 6.67 \cdot 10^{-11} \text{ N} \cdot \text{m}^2 / \text{kg}^2$$

$$M_{\text{sun}} = 1.989 \cdot 10^{30} \text{ kg}$$

$$r_0 = \text{earth's mean distance from Sun} = 1.496 \cdot 10^{11} \text{ m}$$

This gives a mean velocity for earth around the Sun that is

$$v_c = \sqrt{\frac{6.67 \cdot 10^{-11} \text{ N} \cdot \text{m}^2 / \text{kg}^2 \cdot 1.989 \cdot 10^{30} \text{ kg}}{1.496 \cdot 10^{11} \text{ m}}} = 2.98 \cdot 10^4 \text{ m/s} = 29.8 \text{ km/s} \approx 30 \text{ km/s}$$

### **Problem #2: Escape velocity from the sun for an object at 1 AU**

Determine the velocity that an object must achieve to escape from the sun's gravitational attraction to a distance approaching infinity, if it starts at 1 AU from the sun.

Solution:

A mass,  $m$ , must be lifted from an initial distance from the sun,  $r_0$ , to infinity. The force that this effort works against is gravity. Because a force (countering gravity) is exerted through a distance (from  $r_0$  to infinity), work is done on the object. As this work is performed, the object's velocity is gradually reduced from its initial value to a value that must approach zero as the mass recedes to infinity. In effect, all the initial kinetic energy is converted to gravitational potential energy by the process of doing work from  $r_0$  to infinity. Mathematically, this is written as:

---

<sup>6</sup>The equivalence principle postulates that gravitational and inertial masses are equivalent; that is, that the inertial "m" in the first equation is the same as the gravitational "m" in the second equation. No exceptions to the equivalence principle have yet been demonstrated in numerous high-precision experiments, and it plays a crucial role in the theory of general relativity.

$$\begin{aligned} \text{Work} &= \int_a^b \mathbf{F} \cdot d\mathbf{r} = \int_{r_0}^{\infty} \frac{GMm}{r^2} dr \\ &= \left. \frac{-GMm}{r} \right|_{r_0}^{\infty} = \lim_{r \rightarrow \infty} \left( \frac{-GMm}{r} \right) + \left( \frac{GMm}{r_0} \right) = \frac{GMm}{r_0} . \end{aligned}$$

Since this potential energy at infinity represents the total conversion of the object's initial kinetic energy at  $r_0$ , we can equate the initial kinetic energy to this potential energy at infinity:

$$\begin{aligned} \frac{1}{2} m v_e^2 &= \frac{GMm}{r_0} \\ \Rightarrow v_e^2 &= \frac{2GM}{r_0} \Rightarrow v_e = \sqrt{\frac{2GM}{r_0}} \\ \Rightarrow v_e &= \sqrt{2} v_c \\ \Rightarrow v_e \text{ from 1 AU} &\text{ equals } \sqrt{2} \cdot 30 \text{ km/s} = 42 \text{ km/s} \end{aligned}$$

### **Problem #3: Relative velocity of Earth and an object perturbed out of the asteroid belt**

a) If an asteroid belt object in a circular asteroid belt orbit loses orbital energy through a gravitational perturbation (by Jupiter, for example) into a new orbit that has aphelion at the distance of the belt (about 4 AU) and perihelion at 1 AU, and if that object subsequently intersects with the earth at that perihelion point, estimate the relative speed of the meteoroid. Assume that the object has a *prograde* orbit (moves around the sun in the same direction as Earth) in approximately the same orbital inclination as Earth.

b) What if the object is a piece of comet debris, and occupies a *retrograde* orbit (moves opposite to the direction of the earth). Again assume that the meteoroid orbital plane is close to the ecliptic.

#### **Solution:**

a) Since the meteoroid does not quite arrive at the earth from infinity, it must have a perihelion speed (relative to the sun) that is slightly less than  $v_e = 42 \text{ km/s}$  (Problem 2). Since the earth moves at  $30 \text{ km/s}$  around the sun (Problem 1), the relative speed of approach must be slightly less than  $42 \text{ km/s} - 30 \text{ km/s}$ , which is therefore  $v_{\text{relative}} \leq$  about  $12 \text{ km/s}$ .  $10 \text{ km/s}$  might be typical.

b) In this case, the object's speed (relative to the sun) is about  $42 \text{ km/s}$  at 1 AU, but is *added* to the earth's speed of  $30 \text{ km/s}$ , for a relative closing speed of  $72 \text{ km/s}$ . This is faster than the observed speed of approach of most objects. This is an upper limit to the possible atmospheric entry speeds of meteoroids.

### **3.0 METEOROID PHYSICS PRIOR TO THE POINT OF RETARDATION**

As demonstrated by the results of Problems 2-4, above, a meteoroid enters the earth's atmosphere at a speed of, typically, about  $10 \text{ km/s}$ . The meteoroid is then subjected to high thermal and mechanical stresses as it plunges into the atmosphere, resulting in high luminosity and production

of a sonic bow-shock wave. This section describes the physical effects of atmospheric flight at high speeds, ending with relatively slow-speed flight through the terminal phase of flight to the earth's surface.

Notation:

Atmospheric density,  $\rho$ , relative to sea-level density of a standard atmosphere,  $\rho_0$ , as a function of altitude,  $y$ , is modelled reasonably accurately by a mathematical model:

$$\frac{\rho}{\rho_0} = \alpha e^{-\beta y}$$

where  $\alpha = 0.715$  (dimensionless) is the constant of proportionality for a best-fit model of earth's atmospheric density as a function of height, and  $y$  and  $\beta$  are related by the choice of units:

Table I: Value of  $\beta$  depends upon the choice of units for  $y$ :

Units of $y$	$\beta$
ft	1/24,800
mi	1/4.6716
m	1/7,536
km	1/7.536

$r_0$  = earth mean radius =  $6.37 \cdot 10^6$  m

$G$  = newtonian gravitational constant =  $6.67 \cdot 10^{-11}$  N-m<sup>2</sup>/s<sup>2</sup>

$M_E$  = earth mass =  $5.98 \cdot 10^{24}$  kg

$g$  =  $(GM_E/r_0^2)$  = gravitational acceleration at earth's surface = 9.81 m/s<sup>2</sup>

$\rho_0$  = density of earth's atmosphere at sea level = 1.293 kg/m<sup>3</sup>

$\nu$  = Stefan-Boltzmann constant =  $5.67 \cdot 10^{-8}$  J/m<sup>2</sup>·s·K<sup>4</sup>

$\epsilon$  = radiation emissivity of a surface relative to a blackbody ( $\leq 1$ , dimensionless)

$m$  = meteoroid mass, kg

$r_m$  = mean radius of meteoroid, m

$A$  = mean cross-sectional area of meteoroid =  $\pi r_m^2$ , m<sup>2</sup>

$S$  = mean frontal surface area of meteoroid, m<sup>2</sup>, approx  $2\pi(r_m)^2$ , m<sup>2</sup>

$\sigma$  = radius of curvature of meteoroid surface at point(s) where maximum heating occurs, m

$C_D$  = mean coefficient of drag of meteoroid =  $2\sin^2\delta$  for a blunt body of conical half-angle  $\delta$

$C_s$  =  $2.13 \cdot 10^{-4}$  (kg)<sup>1/2</sup> · m<sup>-1</sup>

$V_E$  = entry velocity into the atmosphere = between  $5 \cdot 10^3$  m/s to  $1.2 \cdot 10^4$  m/s, typically  $10^4$  m/s

$\theta_E$  = entry angle into the atmosphere relative to local horizontal, between 0° to -90°

It is fortunate for this discussion that the problem of high-speed entry into the earth's atmosphere has been extensively analyzed in connection with the problems of safely returning manned and

unmanned spacecraft modules from orbit and from trips to the moon. The problem has also been extensively studied in connection with the development of ballistic missile warheads.<sup>7</sup>

I will not derive most of the equations presented in this Section, as such derivations are too lengthy for this presentation. Detailed derivations may be found in References [1-3]. I present here the analytically derived equations that describe entry of objects into earth's atmosphere at high speed, and I plot the results of those equations for typical set of meteoroid parameters. In this section the reader is provided with analytical solutions to such questions as:

- At what altitude does a meteoroid begin to decelerate?
- How does meteoroid velocity vary with altitude?
- How does a shallow atmospheric trajectory differ from a steeply inclined trajectory?
- How large are the maximum dynamic forces (g-forces) that a meteoroid experiences in the atmosphere?
- How do dynamic forces (g-forces) vary with altitude? How do they vary with entry angle into the atmosphere?
- How much radiant energy is produced per unit time and per unit area of a meteoroid's surface?
- How does radiant energy production vary with entry angle into the atmosphere? How does it vary with meteoroid mass? How sensitive is it to meteoroid entry speed?
- How hot does a meteoroid/fireball surface become? Why does it seem to dim so suddenly?
- Can I create a scenario for a "typical" meteoroid flight through the atmosphere, analyzing, among other things, the sequence of initial surface temperature increase, initial deceleration, maximum radiant energy production, maximum g-force loading, and transition to sub-sonic flight?
- How far will meteoroid pieces travel beyond the point of retardation? This is very important for locating a probable fall location.
- Why do the largest pieces of an exploded meteoroid travel to the far end of the strewnfield?

**Figure 1.** Forces acting on a body entering earth's atmosphere from space.

---

<sup>7</sup>There are many technical references for this body of work, but one that is especially readable while remaining technically substantial is Chapter 13 of *Space Technology*, as referenced in the Bibliography. That chapter, *The Possibility of a Safe Landing*, by Alfred J. Eggers, Jr., then of the Ames Aeronautical Laboratory (later NASA-Ames Research Center), underpins much of the mathematical basis of this section.

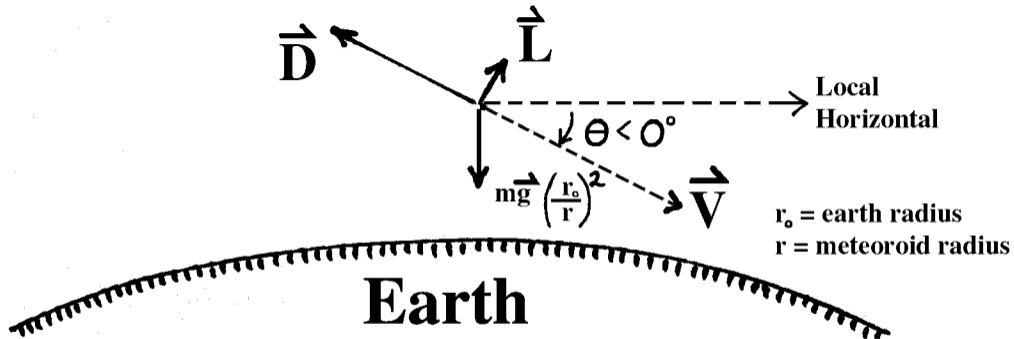


Figure 1. Forces acting upon a meteoroid.

Figure 2. Meteoroid velocity as a function of entry angle and altitude.

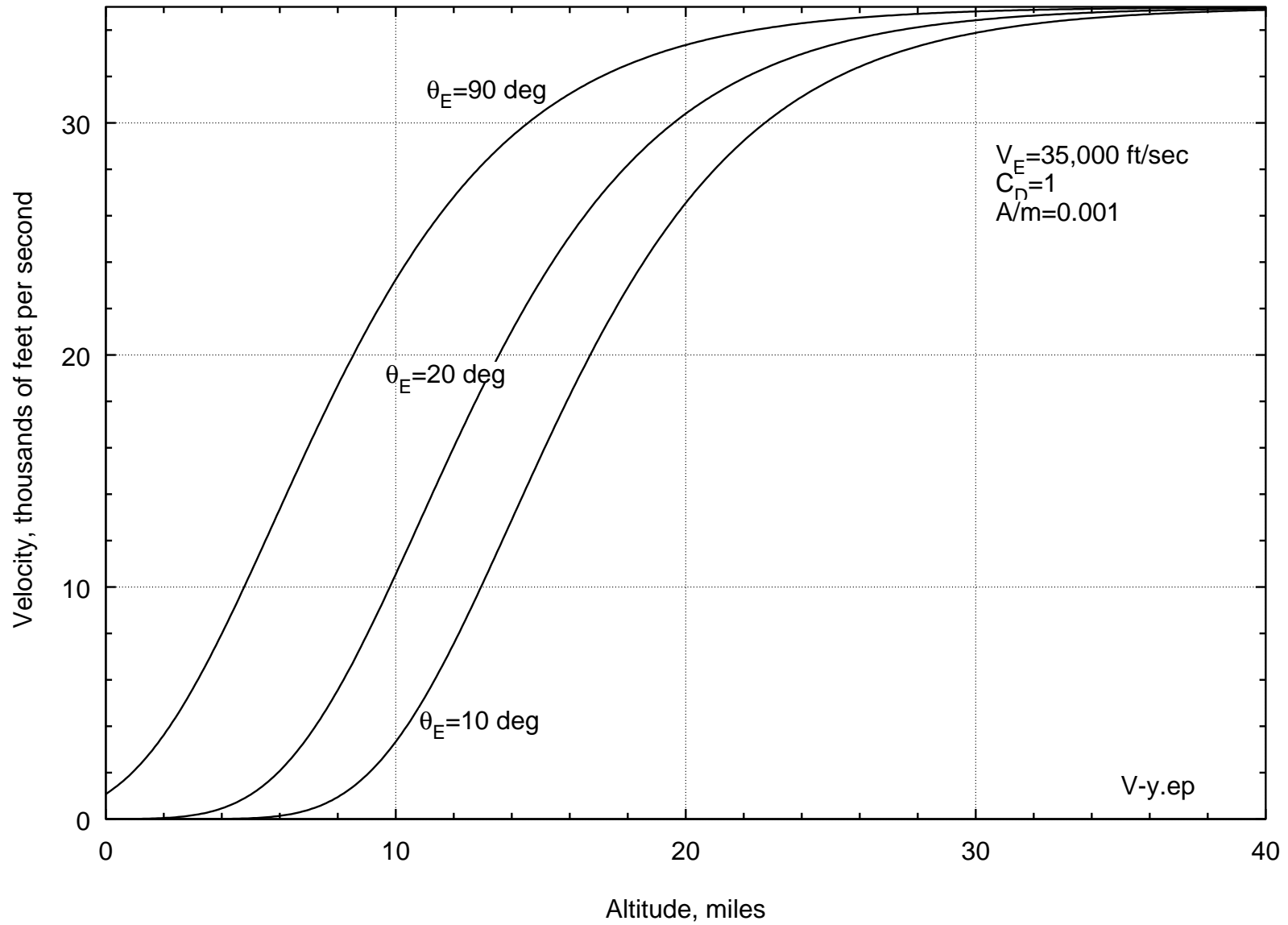
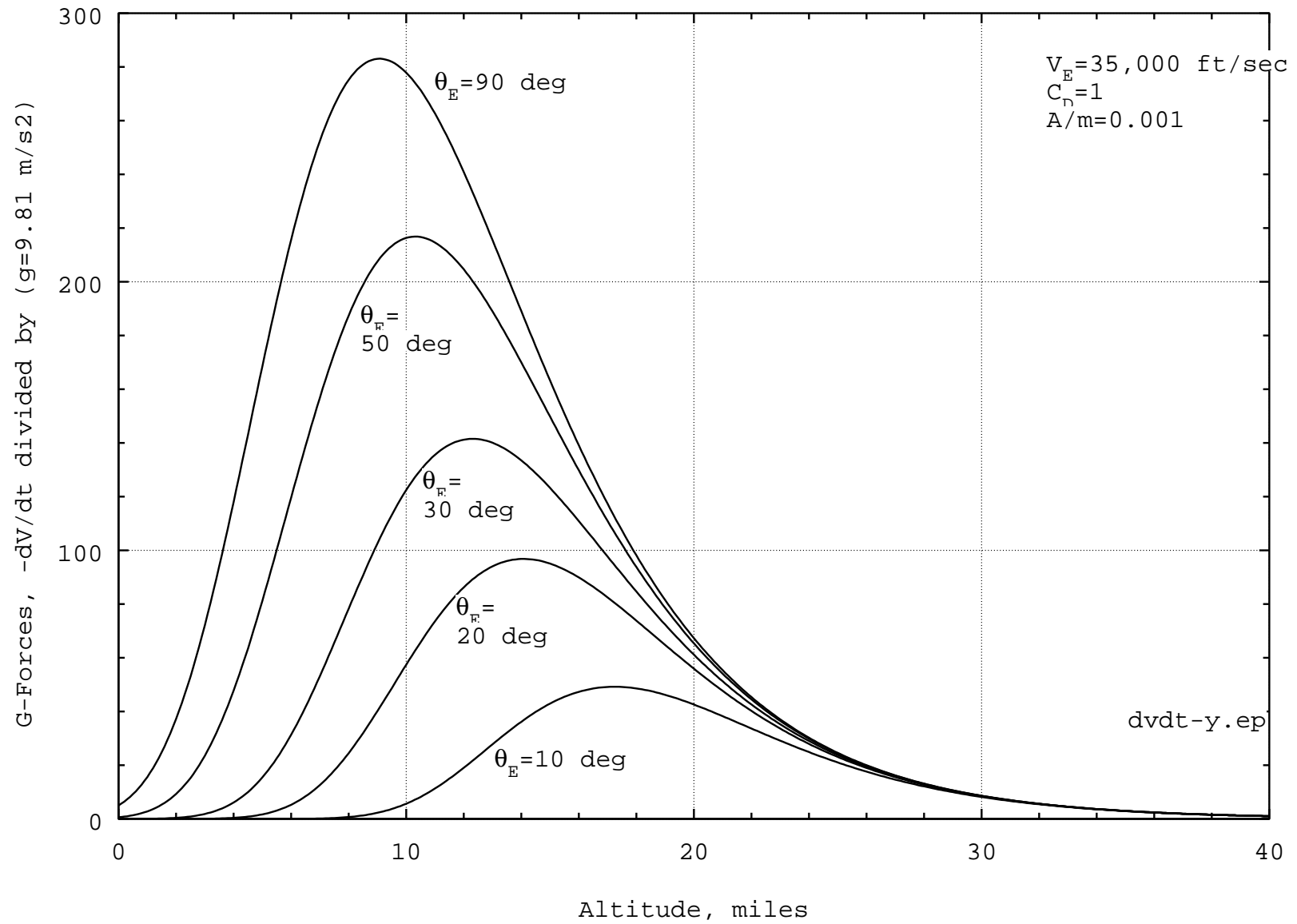


Figure 3. G-forces as a function of entry angle and altitude.



### 3.1 Force balance for atmospheric entry

With reference to Figure 1, the forces acting on an object that enters the earth's atmosphere are as follows:

$$\text{Force balance along direction of object's motion: } L - mg \left( \frac{r_0}{r} \right)^2 \cos\theta = - \frac{mV^2}{r_c}$$

$$\text{Force balance at right angles to object's motion: } D + mg \left( \frac{r_0}{r} \right)^2 \sin\theta = - m \frac{dV}{dt}$$

Where the entry angle,  $\theta$ , is measured relative to the local horizontal, and is always less than zero.

### 3.2 Meteoroid velocity and deceleration during atmospheric flight

For an object that is entering the atmospheric ballistically, the motion is nearly linear through almost the entire flight, and drag due to atmospheric friction is the dominant physical interaction through most of the flight. The force of gravity is insignificant as a factor during this type of flight. [1] analyzes this case in detail, and derives an expression for velocity during the atmospheric flight (with  $\theta$  always less than zero):

$$V = V_E \exp \left[ \frac{C_D \rho_0 A \alpha}{2\beta m \sin\theta_E} e^{(-\beta y)} \right]$$

The deceleration (as fraction of earth's surface gravity, the so-called g-force) of a meteoroid is:

$$- \frac{dV/dt}{g} = \frac{C_D \rho_0 A \alpha V_E^2}{2mg} e^{(-\beta y)} \exp \left[ \frac{C_D \rho_0 A \alpha}{\beta m \sin\theta_E} e^{(-\beta y)} \right]$$

The maximum deceleration experienced by a meteoroid is:

$$- \left( \frac{dV/dt}{g} \right)_{\max} = - \frac{\beta V_E^2 \sin\theta_E}{2ge}$$

The minus (-) sign in front of  $(dV/dt)/g$  indicates that the direction of the deceleration is opposite the direction of a meteoroid's motion. The altitude at which maximum deceleration occurs is:

$$y = \frac{1}{\beta} \ln \left( - \frac{C_D \rho_0 A \alpha}{\beta m \sin\theta_E} \right)$$

and the velocity at which maximum g-forces are experienced is:

$$V_{\max \text{ g-force}} = \frac{1}{\sqrt{e}} V_E \approx 0.61 V_E$$

### 3.3 Analysis of meteoroid velocity and deceleration

From inspection of the equations above, we can observe that:

- For a given value of the drag coefficient, a meteoroid's velocity at any given altitude is determined by the initial entry speed,  $V_E$ , the entry angle,  $\theta_E$ , and the ratio of the meteoroid's cross-sectional area to the meteoroid's mass,  $A/m$ . Higher velocities through the atmosphere are maintained for meteoroids that enter at steep angles and that have lower ratios of  $A/m$ . Geometrically,  $A/m$  decreases as an object's size is increased (see Table II), assuming that the density remains constant. Therefore, smaller meteoroids will move more slowly at any given altitude than larger meteoroids, all other factors being held constant. In other words, more massive meteoroids are slowed down less than smaller meteoroids as they plunge through the atmosphere (Figure 2).

Table II. Geometric relationship between cross-sectional area and mass,  $A/m$ , assuming constant density,  $\rho = 2\rho_{\text{water}} = 2000 \text{ kg/m}^3$ ; and approximately spherical shape.

Mass, m (kg)	Volume, V (m <sup>3</sup> ): $V = \frac{m}{\rho}$	Radius, r (m): $r = \sqrt[3]{\frac{3V}{4\pi}}$	Cross-section area, A (m <sup>2</sup> ): $A = \pi r^2$	Frontal surface area, S (m <sup>2</sup> ): $S = 2\pi r^2 A/m$ (m <sup>2</sup> /kg): $\frac{A}{m} = \frac{3}{4\rho r}$	
1	$5 \cdot 10^{-4}$	$4.9 \cdot 10^{-2}$	$7.5 \cdot 10^{-3}$	$1.5 \cdot 10^{-2}$	$7.5 \cdot 10^{-3}$
10	$5 \cdot 10^{-3}$	0.1061	$3.6 \cdot 10^{-2}$	$7.2 \cdot 10^{-2}$	$3.6 \cdot 10^{-3}$
100	$5 \cdot 10^{-2}$	0.229	0.16	0.32	$1.6 \cdot 10^{-3}$
1000	0.5	0.49	0.75	1.5	$7.5 \cdot 10^{-4}$
10,000	5	1.061	3.6	7.0	$3.6 \cdot 10^{-4}$

For the purposes of making graphs (Figures 2-8) for this analysis, a value of  $1 \cdot 10^{-3}$  is assumed for the  $A/m$  ratio.

- g-forces at any altitude depend upon initial entry speed,  $V_E$ , entry angle,  $\theta_E$ , and the  $A/m$  ratio. The equation is especially sensitive to the entry speed and entry angle.
- Maximum g-forces depend solely upon the entry angle and the entry speed, and are especially sensitive to the entry speed. Maximum g-forces do not depend upon the  $A/m$  ratio. This is an important observation, since the likelihood that a meteoroid will break up in flight increases with higher g-forces. Put another way, meteoroids that enter the atmosphere at higher speeds and steeper entry angles are more likely to break up in flight than equivalent objects entering at lower speeds and more shallow angles.
- Maximum g-forces occur at altitudes between about 7 km to 30 km (4 miles to 20 miles) (Figure 3), depending upon the  $A/m$  ratio. The larger the meteoroid, the lower the altitude at which maximum g-forces occur. Since a meteoroid is likely to experience structural

break-up at or near the moment of maximum dynamic loading, this implies that, if a meteoroid breaks up in flight, the break-up will likely occur within this altitude range.

- Maximum g-force varies between about 50-300 g's, depending sensitively upon both the entry angle and the initial velocity. Thus, a meteoroid is much more likely to reach the ground in one piece if it enters at a shallow angle and a relatively slow speed. But note that a meteoroid falling to earth from the asteroid belt at 11 km/sec and entering the atmosphere at a -10° angle still experiences 50 g's (Figure 3). This result can explain why stony meteoroids rarely reach the ground in one piece, regardless of their entry parameters.

**Problem #4: How do astronauts return through the atmosphere after a trip to the moon?** Astronauts returning to the earth from the moon approach the earth at or near escape velocity, about 10-12 km/sec. Re-entry through the earth's atmosphere must occur at a substantially slower speed, because neither the crew nor the spacecraft could likely survive the 50-300 g's that they would experience if they entered the atmosphere at full speed. But it is impractical to carry enough chemical propellant in the spacecraft to slow down to a velocity that would allow atmospheric entry with low g-forces, assuming that the deceleration was accomplished solely with a chemical de-orbit rocket engine.<sup>8</sup> The question then is, how does the spacecraft slow down enough for safe re-entry?

**Solution:** The returning space vehicle is guided into the atmosphere on a shallow-angle trajectory that causes it to lose a significant amount of energy in the form of heat while it is in the upper atmosphere. The spacecraft is designed and guided so as to generate lift that then sends it back toward space, but now with much-reduced kinetic energy. The spacecraft then enters the atmosphere again, but this time at a much slower speed, a speed that provides for a safe maximum g-force in the lower atmosphere (Figure 4). This is called a *skip-trajectory*.

**Figure 4.** A skip-trajectory for low-g atmospheric re-entry.

---

<sup>5</sup> Braking with chemical propellant requires the loss of propellant mass. Using the subscripts i and f to denote initial and final conditions for spacecraft mass and velocity, the ratio of initial to final mass for a de-orbit rocket burn is:

$$\frac{m_i}{m_f} = e^{(V_i - V_f)/V_e}$$

where  $V_e$  is the propellant exhaust velocity, which is typically about 3,000 m/s. To reduce speed from the initial value of 12 km/sec to a safe speed (in terms of g-forces to which the astronauts are subjected on re-entry) of, say, 4 km/s, would require a mass ratio of  $\frac{m_i}{m_f} = e^{(12,000 - 4,000)} = 14.4$ , implying that about  $13/14 = 92\%$  of the spacecraft's mass would have to be ejected in the form of spent fuel at that point in the flight. Engineering considerations make it impractical to carry so much fuel at that point in the flight, so a simple de-orbit burn is not a feasible possibility for returning lunar astronauts.

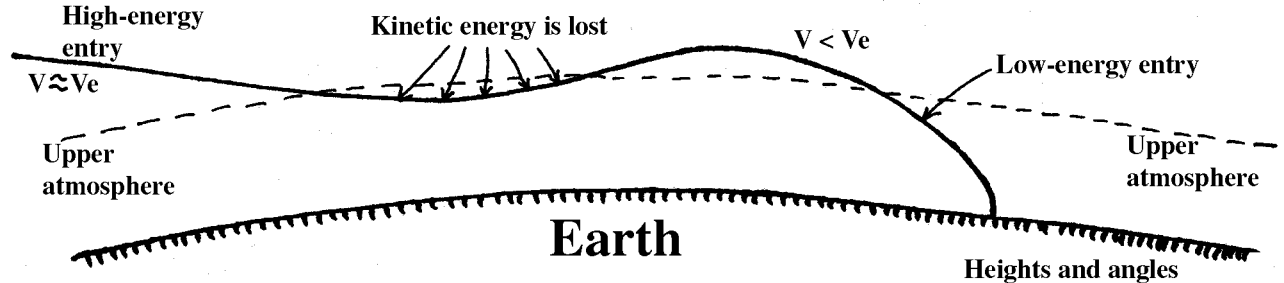


**Figure 4.** A skip-trajectory for low-g atmospheric entry.

Heights and angles  
exaggerated for clarity

Figure 5. Radiant energy production as a function of entry angle and altitude

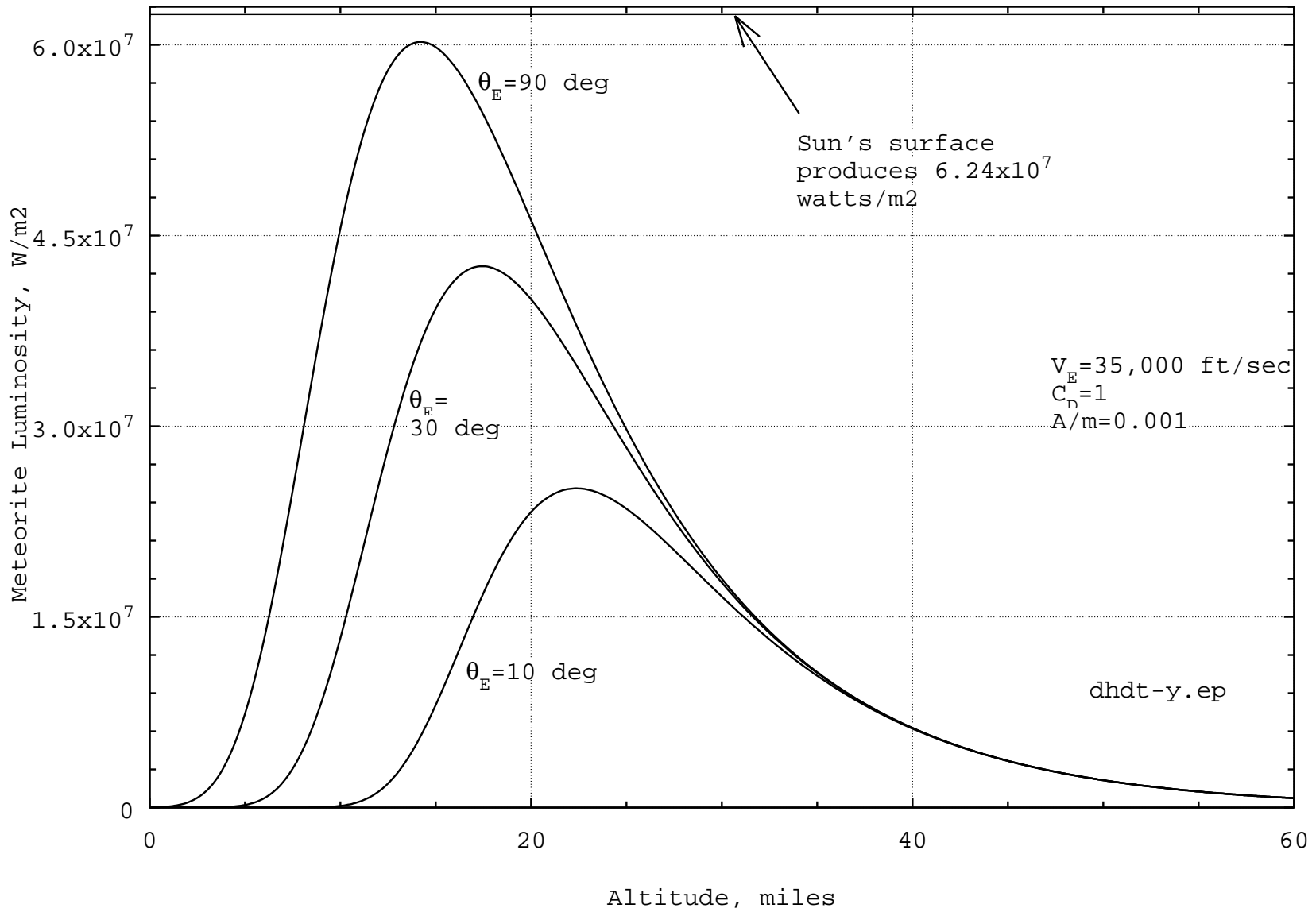


Figure 6. Heating as a function of entry angle ( $\theta_E$ ) and altitude.

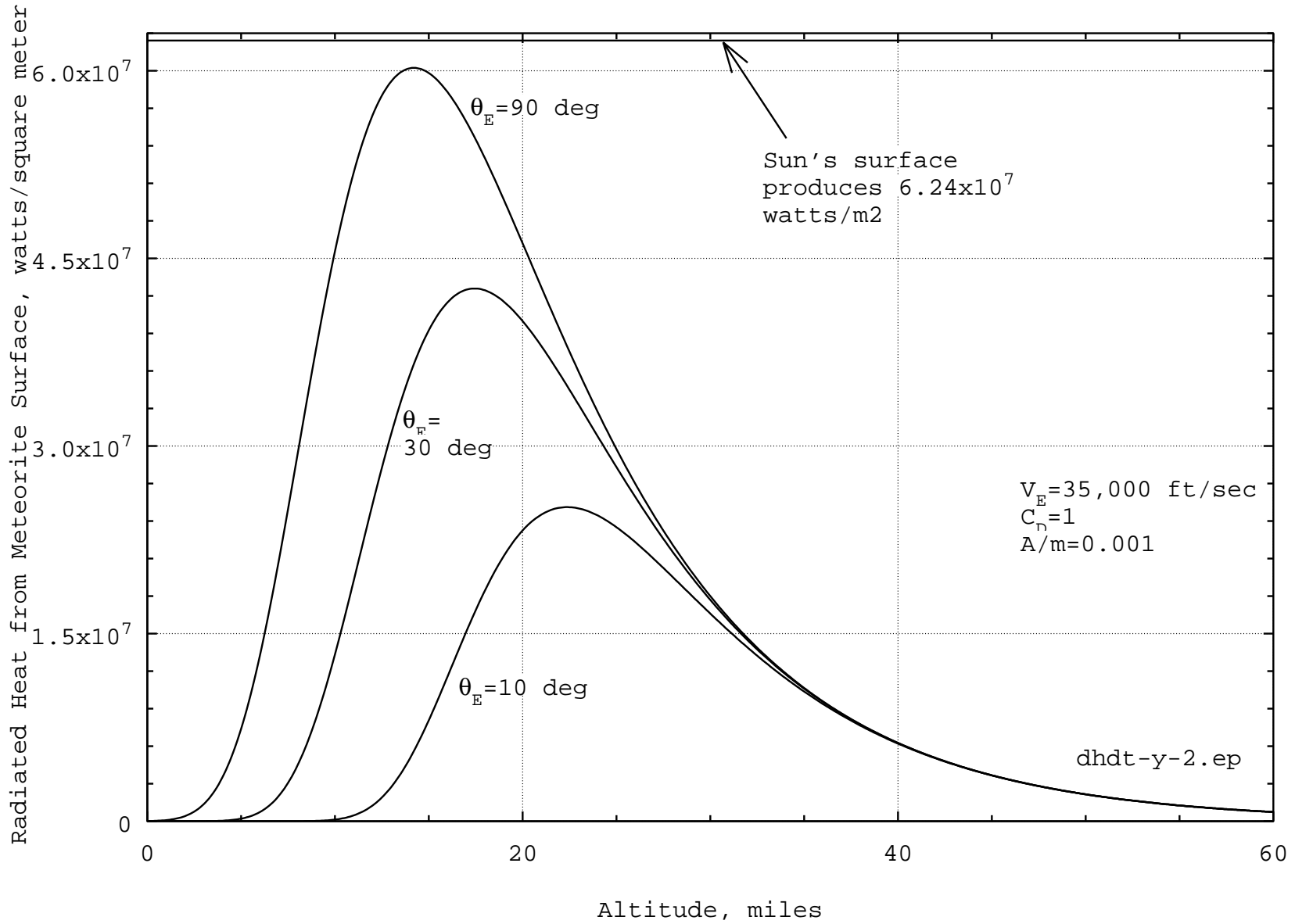


Figure 7. Meteoroid surface temperature as a function of altitude.

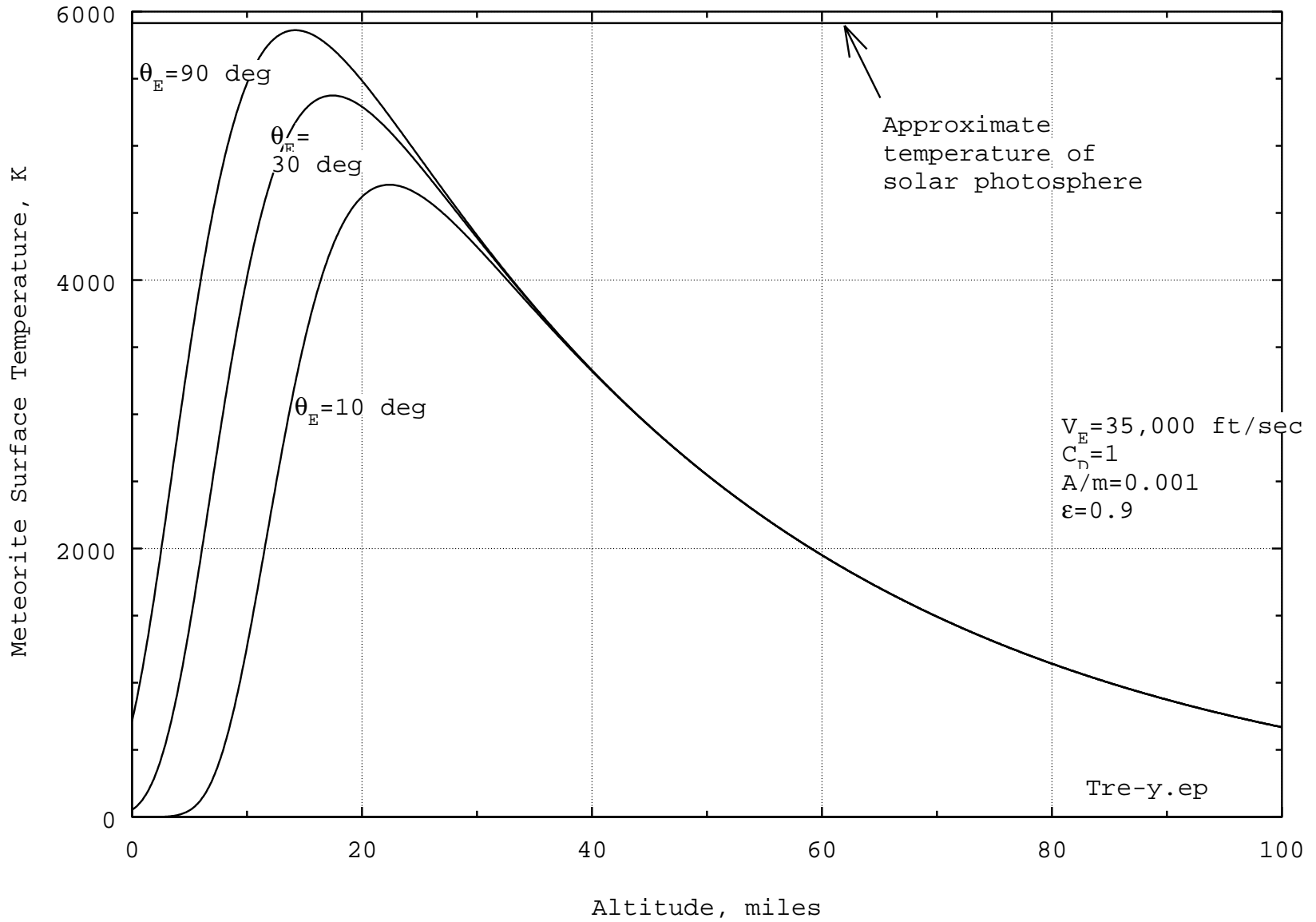
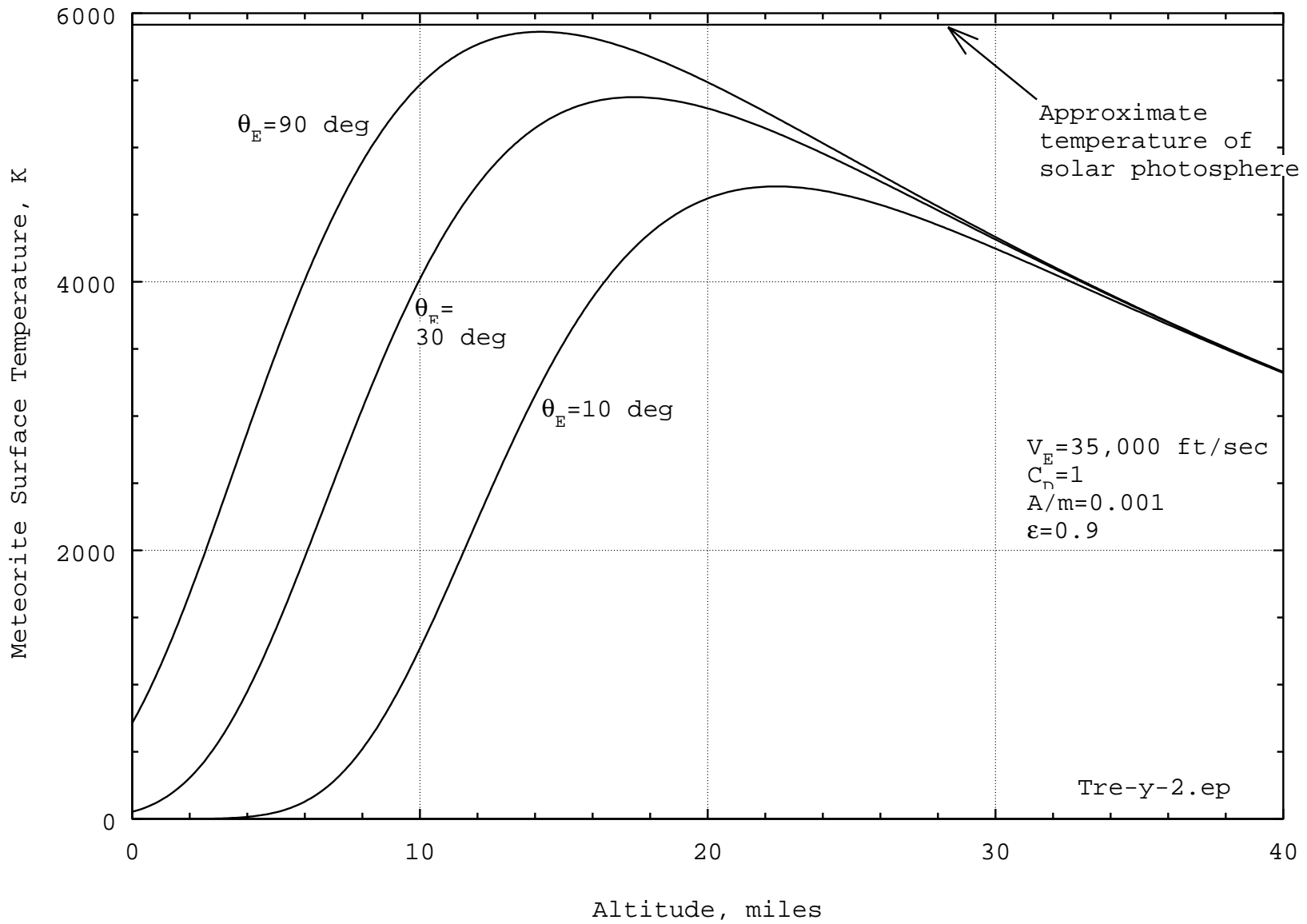


Figure 8. Detail of meteoroid surface temperature during atmospheric flight



### 3.4 Meteoroid energy production and fireball temperature during atmospheric flight

[1] and [2] provide derivations for the heating that an object entering the atmosphere experiences. Heating is due to atmospheric friction, and depends upon atmospheric density ( $\rho$ ), meteoroid velocity ( $V$ ), and the radius of curvature of the meteoroid's surface ( $\sigma$ ). If  $H$  represents a quantity of radiant energy, then  $dH/dt$  represents the rate of radiant energy production (that is, the amount of radiant energy per unit time that the meteoroid produces):

$$\frac{dH}{dt} = C_s \sqrt{\frac{\rho}{\sigma}} V^3 = C_s \sqrt{\frac{\rho_0 \alpha e^{(-\beta y)}}{\sigma}} V^3$$

where  $C_s$  is a proportionality constant, equal to  $2.13 \cdot 10^{-4} \sqrt{\text{kg/m}}$ . The maximum rate of radiant energy production is:

$$\left(\frac{dH}{dt}\right)_{\max} = C_s \sqrt{\frac{-\beta m \sin\theta_E}{3e\sigma C_D A}} V_E^3$$

The altitude at which maximum radiant energy production occurs is:

$$y = \frac{1}{\beta} \ln \left( \frac{3C_D \rho_0 A \alpha}{-\beta m \sin\theta_E} \right)$$

and the velocity at which maximum radiant energy production occurs is:

$$V = V_E e^{-1/6} \approx 0.85 V_E$$

The temperature of a fireball "surface" (actually a ball of ionized gas) can be related to the rate of heat production by assuming that a meteoroid behaves like a black-body in accordance with the Stefan-Boltzmann law, with a surface emissivity,  $\epsilon$ , slightly less than ideal (assume  $\epsilon = 0.9$ ):

$$v\epsilon T^4 = \frac{dH}{dt} \Rightarrow T = \sqrt[4]{\frac{1}{v\epsilon} \frac{dH}{dt}}$$

### 3.4 Analysis of equations for energy production and "surface" temperature

From inspection of these equations, we can observe that:

- Maximum radiant energy production rate is mainly a function of entry velocity, with a relatively small dependence on entry angle and  $A/m$  ratio. Changing entry angle from  $-10^\circ$  to  $-90^\circ$  only changes maximum heating production rate by a factor of  $\sqrt{(\sin 90/\sin 10)} = 2.4$ , and changing  $m/A$  by a factor of 10 changes the maximum heat production rate by a factor of only  $\sqrt{10} = 3.3$ . As meteoroid size increases,  $m/A$  goes up as the mean radius,  $r$ , of the meteoroid, so the maximum heat production rate only increases as  $\sqrt{r}$  if the meteoroid density remains constant. The maximum heat production rate is very sensitive to  $V_E$ , changing as the cube of that quantity.

- The altitudes of maximum surface heating and maximum g's are usually between 14 km to 30 km (8 miles to 20 miles) above the earth's surface. However, detailed analysis shows that maximum heating does slightly precede maximum deceleration (compare Figure 3 to Figure 5).
- Maximum luminosity (radiant energy production per unit time per square unit of surface area) approaches that of the sun. As shown in Figure 5, peak luminosity for a -90° entry angle at 11 km/s is nearly the same as solar luminosity, perhaps 60 million watts per square meter of surface. For -10° entry angle at 11 km/s, the luminosity is still half as great as that of the sun. This explains why fireballs are so bright.
- Surface heating begins before substantial deceleration occurs. As shown in Figure 6, the heat production from a meteoroid surface begins at about 60 miles altitude, and is about 750,000 watts/m<sup>2</sup> when the object reaches 40 miles altitude. Compare this to Figure 2, which shows that almost all deceleration occurs below 40 miles altitude.
- Meteoroid surface temperature almost always peaks at about 5000 degrees kelvin, the same as the sun's visible surface. Maximum meteoroid surface temperature is relatively insensitive to a meteoroid's physical parameters because it varies as the fourth root of the heat production rate. As shown in Figures 7 and 8, surface temperature begins to increase when the meteoroid is still above 160 km (100 miles) altitude, and reaches a peak between about 15-30 km (10-20 miles) altitude. The surface temperature of 5000 K is approximately the same as that of the sun's visible surface, the photosphere.
- Meteoroid heat production and surface temperature decrease very rapidly at altitudes below about 10 miles. This is shown on the curves in Figures 5-8. This explains why meteoroid point of retardation is usually at or above 8-10 miles. When the meteoroid drops below that altitude, its radiant energy production and temperature drop below the minimum necessary to make the object shine brightly at visible-light frequencies. With reference to Figure 2, this is also the altitude range at which meteoroid forward velocity drops to nearly zero for shallow entry angles.

**Problem #5: Treating fireballs as approximate blackbodies, and using Wien's displacement law, calculate the altitude range within which fireballs should**

**typically be visible:** Wien's displacement law states that the wavelength,  $\lambda$ , of peak radiation from a blackbody object at a temperature, T, is:

$$\lambda = \frac{2.898 \cdot 10^{-3} \text{ m K}}{T}$$

where  $\lambda$  is in meters and T is in degrees kelvin. The wavelengths to which the human eye is sensitive are about  $500 \cdot 10^{-9}$  m (blue light) to  $625 \cdot 10^{-9}$  m (red light).

- If a fireball is treated as a blackbody, to what temperature range does this correspond?
- Using the curves of Figures 6-7, determine the altitude range within which fireballs should be visible. What is the altitude range for point-of-retardation?

**Solution:** The blue extreme corresponds to  $T=2.898 \cdot 10^{-3}/\lambda$ , and the red extreme corresponds to  $T=2.898 \cdot 10^{-3}/\lambda$ . Plugging in the values for  $\lambda$  given in the problem statement gives a temperature range of 5,800 K to 4,600 K. Thus, the low-temperature cut-off below which a blackbody will not be visible to the human eye is about 4,600 K. The curves of Figures 6-7 exceed this

temperature at altitudes of about 8-30 miles. Thus, it is likely that fireballs will not be visible at altitudes above 30 miles, while the low-temperature cut-offs for the left-hand sides of the curves range between 8-20 miles, implying that this is the range of altitudes for the point-of-retardation.

**Problem #6: How to track a meteoroid after it has passed the point of retardation:**

After the meteoroid is no longer seen to emit bright light that is visible to human eyes, how could a meteoroid's emissions be tracked? How can high-altitude meteoroids be observed?

Solution: Consider a meteoroid to behave approximately as a blackbody. After it reaches the point of retardation, its heat production rate can no longer keep it hot enough to emit visible light, but its surface temperature is still close to 4600 K at that point, and cools gradually as it falls, dropping to perhaps 500 K or less before it hits the ground, as shown in Figure 7. By Wien's displacement law (see Problem #5), this 500-4600 K temperature range will cause the meteoroid to produce infrared (heat) radiation after it passes the point of retardation. Stated simply, the rock's surface will remain hot for some time after it passes the point of retardation. Therefore, infrared (heat)-sensitive detectors should be able to track a meteoroid after it becomes invisible to human eyes. Infrared detectors can also be used to observe meteoroids at high altitudes, before they are sufficiently hot to emit visible-light radiation.

- Ablation effects are explained by meteoroid radiant-energy production, surface temperature, and convective flow. As shown in a graph in Norton, a large fraction of a meteoroid's mass may be lost due to *ablation* effects. Ablation is the loss of surface material due to extreme heating that loosens surface material, and subsequent stripping of that material due to convective flow around a body. As quickly as old surface material is heated and lost, the newly exposed surface is also heated and lost. This ablation process continues until the meteoroid surface temperature and dynamic forces decrease sufficiently. The final layer of burned-looking surface, the *fusion crust*, represents the final, heated meteoroid surface that chilled before being stripped away.
- The luminous fireball is explained by meteoroid radiant-energy production. Atmospheric gases flowing convectively around the meteoroid gain energy due to the meteoroid's radiant output. These gases become hot as a result, and re-radiate the energy. These gases form the fireball that is visible to witnesses. The fireball diameter is much larger than the meteoroid diameter. The fireball gases are *ionized*, meaning that their atoms are stripped of some of their electrons, and thus form a *plasma*.
- The moving fireball plasma is probably the source of electrophonic "sound." Many eyewitnesses to fireballs report that they hear buzzing, whooshing, whirring, or clicking sounds simultaneously with the visible event. Since they are located too far from the fireball to hear acoustic energy simultaneously with the event, they are evidently "hearing" some sort of electromagnetic phenomenon. It is likely that the source of the "sound" is audio-frequency radio energy that is generated by movement of the ionized fireball plasma through the earth's magnetic field lines. Although human beings cannot perceive such energy directly, a plausible hypothesis is that they can hear the acoustic effects that occur when such radio energy encounters, and causes vibration of, nearby metal and electrical devices such as power lines and power transformers.

### 3.5 Meteoroid sound effects

Meteoroids produce three distinct types of acoustic energy during flight: Explosion waves, sonic bow shock waves, and low-amplitude sounds that are not currently understood. *Acoustic waves from explosion events* are probably generated by break-up of meteoroids at or before maximum dynamic loading due to dynamic forces of deceleration. The wavefronts from these events move isotropically away from the meteoroid, and thus can be heard by any nearby witnesses.

*Sonic bow shock waves* are generated as shown in Figure 9. The wavefront produced by individual wavelets along the path of the fireball's flight moves at the speed of sound. If this bow shock moves past a witness, the person will hear a sonic boom.

**Figure 9.** Sonic bow shock wave formation from spherical wavelets.

**Problem #7: Angle of the bow shock wave, and why a zone of silence exists for some witnesses.** As shown in Figure 9, the bow shock can be modelled as a series of wavelets, the cumulative wavefront of those wavelets forming the wave. The bow shock thus forms a cone, which is seen in cross-section in the Figure. The half-angle of the cone (the angle between the surface of the cone and the meteoroid's line-of-flight) can be calculated by observing that the radius of each wavelet is at a right angle to the conical bow-shock wavefront. The wavelet radius and the bow shock from the end of the radius to the meteoroid form two legs of a right triangle, and the meteoroid's flight line makes the hypotenuse of the triangle. The length of the radius is  $\Delta t \cdot v_s$ , and the length of the hypotenuse is  $\Delta t \cdot v_m$ , where  $\Delta t$  is arbitrary,  $v_s$  is the speed of sound, and  $v_m$  is the speed of the meteoroid. Thus, by inspection, the half-angle,  $\theta$ , of the Mach cone is determined to be:

$$\theta_{\text{half-angle Mach cone}} = \arcsin\left(\frac{v_s}{v_m}\right)$$

For meteoroid speeds that are many times faster than sound, the half-angle is a few degrees. For example, at twenty times the sea-level speed of sound (approximately 6.6 km/s), the bow shock angle is  $2.9^\circ$ . At ten times the sea-level speed of sound (approximately 3.3 km/s), the bow-shock half-angle is  $5.7^\circ$ . (*Note that speed of sound varies with temperature and pressure, and thus with altitude, complicating precise calculations for any given bolide event.*)

The bow shock wave moves away from the fireball's line-of-flight at nearly right angles to that flight path. Direction-of-arrival of the bow shock wave at a listening station is therefore a good, but not exact, indicator of the fireball's flight track heading. But observers who are ahead of the fireball's flight will not hear the bow-shock, precisely because of its right-angle propagation relative to the fireball flight path.

Because meteoroids are subjected to high (50-300) g-forces during flight, they are likely to break up in flight, especially if they have a stony composition. These break-ups are apparently quite energetic in some cases, as evidenced by the production of explosion sounds in connection with such events. Explosion sounds radiate *isotropically* (equally in all directions), and can thus be

heard by all nearby observers. Because they radiate isotropically, their direction-of-arrival at listening stations does not yield information on fireball flight track heading.

A third type of meteoroid sound is picked up by low-frequency (infrasound) acoustic listening stations, and is produced by a process that is not yet understood. These sounds may possibly be caused by a wake vortex behind meteoroids, or possibly by the tumbling of meteoroids.

### 3.6 Uses of meteoroid sounds

Acoustic energy, if received at infrasound monitoring stations, can be used to determine fireball heading, fireball ground track, and the locations of possible strewnfields below the fireball trajectory.

- 1) Fireball heading: Bow shock waves are produced at approximately right angles to meteoroid flight. If direction-of-arrival of a bow shock wave is known, then approximate fireball flight heading can be determined. Ground track can be determined with multiple listening stations if they are operated on a common timebase.
- 2) Strewnfield locations: If the location of an explosion can be triangulated from multiple listening stations, then a possible strewnfield can be approximated relative to the explosion location.
- 3) Determination of fireball ground track: Locations of multiple explosions can be triangulated, and the line connecting the explosions can be taken as the fireball ground track. Bow shock waves can also generate this information, if precise time-of-arrival at multiple listening stations is determined.

Table III. Uses for meteoroid sounds.

	Fireball flight heading	Fireball ground track	Strewnfield location
Bow shock wave direction-of-arrival	Can be determined approximately, using direction of arrival at a single station.	Can be determined approximately using multiple stations on a coordinated timebase.	No.
Explosion acoustic wave direction-of-arrival	Can be determined approximately, if multiple stations record direction-of-arrival of multiple explosion events.	Can be determined approximately, if multiple stations record direction-of-arrival of multiple explosion events.	Only if strewnfield is associated with an explosion event.
Wake vortex acoustic signal (?)	(?)	(?)	No.

### 3.7 Detection of meteoroids using infrasound stations

The United States government operates a network of infrasound stations. Early development work on these stations was performed at the Department of Commerce (DOC) laboratories in Boulder, Colorado in the 1960's. The stations were designed to detect acoustic energy from nuclear explosions in Asia. The development was successful. Subsequent to the original development efforts, the infrasound program split into two parallel efforts, one military-sponsored and the other sponsored through the DOC. The military-sponsored effort was subsequently subsumed by the Department of Energy (DOE) Los Alamos National Laboratory (LANL). The DOC effort, under the National Oceanic and Atmospheric Administration (NOAA) now operates a single station near Erie, Colorado. The LANL network utilizes stations at locations in the United States and abroad.

Shock wave propagates at right angles to meteoroid flightline.

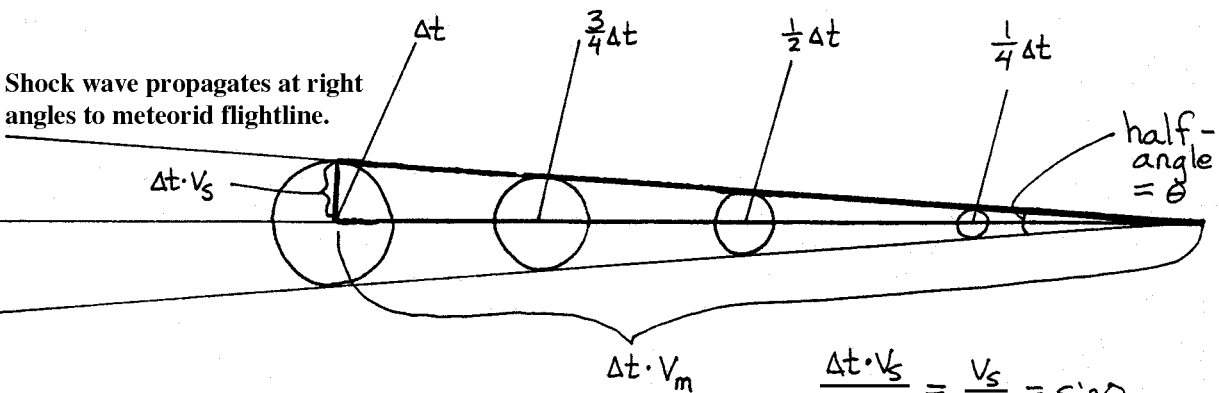


Figure 9. Geometry of meteoroid bow-shock wave front.

$$\frac{\Delta t \cdot V_s}{\Delta t \cdot V_m} = \frac{V_s}{V_m} = \sin \theta$$

Verification of adherence to the Total Nuclear Test Ban Treaty (assuming that the U.S. Senate ratifies it) will require the use of the LANL network. Data from the network on fireball events have been released in the past, and presumably will continue to be released in the future. The DOC infrasound station has also generated useful public-domain information on fireball acoustic events.

### 3.8 Detection of meteoroids using satellites

The United States government operates a network of satellites to provide early warning and tracking of rocket launches. The same satellites are also designed to detect and assess large explosion events, both nuclear and non-nuclear. The satellites are operated under the Department of Defense (DOD) Defense Support Program (DSP) [3a] and the Satellite-Based Infrared System (SBIRS). The satellites occupy geosynchronous orbits, from which they hover over (approximately) fixed locations on the Earth's surface. The satellites utilize telescopes that focus energy on infrared detectors. The telescopes have small fields of view, but the satellite mission requires wide-area surveillance. Therefore the DSP telescopes are scanned conically across the Earth's surface from each satellite location. The result is that any given point on the Earth's surface is observed not continuously, but rather at intervals of between 6 to 10 seconds [3b], depending upon the particular satellite. Bright meteoroids are routinely detected by DSP satellites, and coordinates and altitudes of points along the flight tracks of those meteoroids can be determined from DSP data. Unclassified data can be, and have been, released by DOD through LANL. But a meteoroid flight track cannot be determined from DSP data unless the meteoroid flight lasts long enough for the DSP to see it on at least two rotational scans. This means that the bright portion of the meteoroid flight must exceed 6 to 10 seconds if DSP data are to yield a flight track. This is longer than most fireball events. However, even a single DSP data point can be very useful to fireball researchers, because the high accuracy of a single DSP point serves to constrain the flight track as determined from all other available information sources and witnesses.

## 4.0 METEOROID PHYSICS AFTER THE POINT OF RETARDATION

Point of retardation (POR) is typically between 13-30 km (8-20 mi) altitude (see Problem #5). Within this altitude range, Figure 2 shows that meteoroid forward velocity is close to  $V_E$  at 30 km, but that it is probably between 1-3 times the speed of sound, 330 m/s (1100 ft/s), for a body that reaches the point-of-retardation at an altitude of 13-16 km (8-10 mi), if the body's entry angle is shallow. If the body's entry angle is steep, approaching  $90^\circ$ , then it may still be moving at about half of  $V_E$  when it reaches the point-of-retardation. Because of the disparate meteoroid velocities in these two conditions, these represent two distinct physical cases that have to be considered for meteoroid flight after the POR.

### 4.1 Case #1: Flight after point-of-retardation for a steep entry angle (near $90^\circ$ )

This is the simpler of the two cases to analyze. With reference to Figure 9, a meteoroid has two components of motion, horizontal and vertical, at the moment that it reaches the POR. Neglecting atmospheric resistance, the equations of motion are:

$$\text{Horizontal displacement from POR: } D_x = V_0 t \cos\theta$$

$$\text{Vertical displacement from POR: } D_y = \frac{1}{2} g t^2 + V_0 t \sin\theta$$

A steeply inclined meteoroid will still be moving at close to the speed of sound when it reaches the earth's surface (Figure 2). Thus, the effects of the atmosphere can be neglected for steep angles and high speeds. We calculate from these equations the time,  $T$ , to fall a distance  $A_0$  from the POR to the ground (the time at which  $D_y = -A_0$ ):

$$\frac{1}{2} gT^2 + V_0 T \sin\theta + A_0 = 0$$

which is solved by the quadratic:

$$T = \frac{-V_0 \sin\theta - \sqrt{V_0^2 \sin^2\theta - 2gA_0}}{g}$$

Note that  $\sin\theta < 0$  and  $g > 0$  in this equation.  $D_x = V_0 T \cos\theta$ , or

$$D_x = \frac{-V_0 \cos\theta}{g} \left( V_0 \sin\theta + \sqrt{V_0^2 \sin^2\theta - 2gA_0} \right)$$

Since the first term in the square root is much larger than the second term, the binomial theorem can be used to approximate the square root term in the equation as:

$$-V_0 \sin\theta + \frac{gA_0}{V_0 \sin\theta}$$

This makes the expression for T reduce to:

$$T = \frac{-A_0}{V_0 \sin\theta}$$

so that  $D_x$  becomes, for steep-angle meteoroids, just one leg of a right triangle:

$$D_x \approx \frac{-A_0}{\tan\theta}$$

A meteoroid's flight path will be somewhat altered by atmospheric resistance, so as to result in a slightly smaller horizontal displacement of the fall from the POR than this equation indicates. However, the effect due to the atmosphere will be relatively small for steep-angle events, and in the absence of detailed information on any particular fireball's velocity, the equation above should be used to determine the upper bound on the possible horizontal displacement between the point-of-retardation and the location of a fall for a steep-angle meteoroid.

**Problem #8: Example calculation of  $D_x$  for a steep entry angle:** If  $A_0 = 24$  km (15 mi) and  $\theta = 70^\circ$ , calculate  $D_x$ .

**Solution:** Plugging the numbers into the equation gives  $D_x = 8.9$  km (5.5 mi). Searchers should work on the ground between the spot that is under the POR and the spot described by the displacement,  $D_x$ . In this case, the maximum area to be searched would therefore be an ellipse 8.9 km long, and perhaps half that wide, that is oriented along the fireball's azimuth and that is anchored with one end directly under the POR.

## 4.2 Case #2: Flight after point-of-retardation for a shallow entry (near 10°)

A meteoroid may still be moving at close to the speed of sound when it reaches the point-of-retardation (POR); therefore, it will travel some distance,  $D_x$  horizontally beyond the POR before landing on the earth's surface. As for Case #1, above, the question is how far? This is important information for personnel who are searching for the fall. Unlike the steep-angle case (above), atmospheric effects cannot be ignored for shallow angles. What the question reduces to: What is the path through the atmosphere of a rock that is shot nearly horizontally at about the speed of sound? If no atmosphere existed, then the equations of motion would be those for a particle in free space, projected at an initial velocity  $V_0$  (the velocity at the POR), and an initial angle  $\theta$  relative to the local horizontal and the solution for  $D_x$  would be:

Horizontal displacement from POR:  $D_x = V_0 t \cos\theta$

Vertical displacement from POR:  $D_y = \frac{1}{2}gt^2 + V_0 t \sin\theta$

In the absence of atmospheric effects, the time to fall to earth from the POR at an initial height,  $A_0$ , above the surface is determined by the condition that:

$$A_0 = \frac{1}{2}gT^2 + (V_0 \sin\theta)T$$

which can be solved for T to yield the time of fall:

$$T = \frac{-V_0 \sin\theta + \sqrt{V_0^2 \sin^2\theta + 2gA_0}}{g}$$

where all physical quantities ( $g$ ,  $V_0$ , and  $\theta$ ) in the equations are treated as positive. Designating the height above the ground of the POR as  $A_0$  and the horizontal displacement as  $D_x$ , the horizontal displacement during the fall time from the POR is:

$$D_x = T \cdot V_0 \cos\theta$$

and substituting the equation for T into this equation for  $D_x$  yields:

$$D_x = \frac{V_0^2 \cos\theta \sin\theta}{g} \left( \sqrt{1 + \frac{2gA_0}{V_0^2 \sin^2\theta}} - 1 \right)$$

### **Problem #9: Prove the relations for T and $D_x$**

a) Using the equations of motion for  $D_x$  and  $D_y$ , prove the relations presented above for T and  $D_x$ . Treat all physical quantities ( $V_0$ ,  $A_0$ ,  $\theta$ , and  $g$ ) as positive.

b) For  $V_0=330$  m/s,  $\theta=18^\circ$ , and  $A_0=16$  km, determine the time-of-fall and horizontal displacement in the absence of atmospheric effects. For the 11 January 1998 Kiowa fireball, assume  $V_0=330$  m/s,  $\theta=10^\circ$ , and  $A_0=12.2$  km, and determine the same parameters. Re-calculate for  $V_0=165$  m/s.

Solution: a) Use the quadratic equation and algebraic re-arrangement of terms:

$$\frac{1}{2} gT^2 + (V_0 \sin\theta)T - A_0 = 0$$

$$T = \frac{-V_0 \sin\theta + \sqrt{V_0^2 \sin^2\theta + 2gA_0}}{g} \quad (\text{positive root to yield } T > 0)$$

$$D_x = T \cdot V_0 \cos\theta = \frac{V_0 \cos\theta}{g} \left( \sqrt{V_0^2 \sin^2\theta + 2gA_0} - V_0 \sin\theta \right)$$

$$D_x = \frac{V_0 \cos\theta}{g} \left( \sqrt{V_0^2 \sin^2\theta \left( 1 + \frac{2gA_0}{V_0^2 \sin^2\theta} \right)} - V_0 \sin\theta \right)$$

$$D_x = \frac{V_0^2 \sin\theta \cos\theta}{g} \left( \sqrt{1 + \frac{2gA_0}{V_0^2 \sin^2\theta}} - 1 \right)$$

b) Inserting the given values for the physical parameters and constants for the first non-atmospheric case yields:

$$V_0=330 \text{ m/s: } T = 48 \text{ sec, } D_x = 15 \text{ km}$$

$$V_0=165 \text{ m/s: } T = 52 \text{ sec, } D_x = 8.2 \text{ km}$$

and for the 11 Jan 1998 Kiowa fireball the solution sans atmospheric effects is:

$$V_0=330 \text{ m/s: } T = 44 \text{ sec, } D_x = 14.4 \text{ km}$$

$$V_0=165 \text{ m/s: } T = 47 \text{ sec, } D_x = 7.6 \text{ km}$$

### 4.3 Atmospheric drag effects

Atmospheric drag will significantly reduce this distance for shallow entry angles. To estimate this reduction, it is necessary to first estimate the time required for a meteoroid to fall from the POR to the earth's surface in the presence of atmospheric resistance. If the atmospheric entry angle is shallow, then the meteoroid's vertical component of velocity at the POR is on the order of 100 m/s if the velocity at the POR is on the order of the speed of sound. (For example, if  $V_0 = 330$  m/s and  $\theta = 10$  to 20 degrees, then the vertical velocity component is initially between 57 m/s to 113 m/s.) The vertical component of motion is resisted by the atmosphere, and the vertical velocity will approach a constant speed, at which the force of resistance is equalled by the force of gravity. This is called the *terminal velocity*. At typical terminal velocities in the earth's lower atmosphere, the atmospheric resistance force is proportional to the square of the velocity and linearly proportional to atmospheric pressure, such that:

$$km \left( \frac{\rho}{\rho_0} \right) V_{\text{terminal}}^2 = mg$$

$$V_{\text{terminal}} = \sqrt{\frac{g\rho_0}{k\rho}}$$

where  $k =$  (for a dense, blunt object<sup>9</sup>)  $2.74 \cdot 10^{-4} \text{ m}^{-1}$ .

Since atmospheric pressure within a few tens of kilometers of the earth's surface varies according to the best-fit function:

$$\frac{\rho}{\rho_0} = e^{-\beta y}$$

the terminal velocity varies with altitude,  $y$ , as:

$$V_{\text{terminal}} = \sqrt{\frac{ge^{\beta y}}{k}}$$

**Problem #10: Terminal velocity for a dense, blunt object near the earth's surface and at 16 km altitude:** What is the terminal velocity for a dense, blunt object near the earth's surface? What is the terminal velocity of a dense, blunt object at an altitude of 16 km? How does this speed compare to the initial vertical velocity component at the POR for a shallow-angle meteoroid? Describe verbally how the meteoroid's vertical velocity profile must behave.

**Solution:** Using the appropriate physical quantities, and setting the density ratio equal to unity for altitudes near the earth's surface, the terminal velocity near the earth's surface is 190 m/s. At an altitude of 16 km, where atmospheric density is much reduced (about 0.12 of surface density), the terminal velocity is 547 m/s, about 2.9 times faster than at the earth's surface. Because the terminal velocity at the altitude of a typical POR is much faster than the shallow-angle meteoroid's initial downward velocity, the meteoroid will initially free-fall, accelerating at roughly the rate of  $g$ , until its downward velocity at some altitude approaches the terminal velocity at that altitude. From that altitude to the earth's surface, the meteoroid will move downward at a terminal velocity that will gradually slow as atmospheric pressure increases.

Thus, the meteoroid's time-of-flight can be modelled by assuming free-fall at an acceleration of  $g$  from the POR to the altitude at which the velocity equals the terminal velocity, and then a terminal-velocity descent from that point onward. Because the free-fall portion of the flight can be modelled by equations for velocity,  $V$ , and distance fallen,  $d$ , in terms of time-of-flight,  $t$ :

$$V = gt + V_0 \sin\theta$$

$$d = \frac{1}{2}gt^2 + (V_0 \sin\theta)t$$

---

<sup>9</sup>Derived from the graphs in *Classical Dynamics of Particles and Systems, 2nd ed.*, Jerry B. Marion, Academic Press, 1970, pp. 53-55.

and the velocity as a function of altitude,  $y$ , is determined as follows:

$$t = \frac{V - V_0 \sin \theta}{g}$$

$$d = \frac{1}{2} g \frac{(V - V_0 \sin \theta)^2}{g^2} + \frac{(V_0 \sin \theta)(V - V_0 \sin \theta)}{g}$$

$$d = \frac{V^2 - 2VV_0 \sin \theta + V_0^2 \sin^2 \theta}{2g} + \frac{2VV_0 \sin \theta - 2V_0^2 \sin^2 \theta}{2g}$$

$$d = \frac{V^2 - V_0^2 \sin^2 \theta}{2g}$$

and substituting  $(A_0 - y)$  for  $d$  and solving for  $V$  gives:

$$V = \sqrt{2g(A_0 - y) + V_0^2 \sin^2 \theta}$$

Since the terminal velocity varies with  $y$  as:

$$V_{\text{terminal}} = \sqrt{\frac{ge^{\beta y}}{k}}$$

The altitude at which the free-fall velocity equals the terminal velocity is given by the value of  $y$  that satisfies the relation:

$$\sqrt{2g(A_0 - y) + V_0^2 \sin^2 \theta} = \sqrt{\frac{ge^{\beta y}}{k}}$$

Since this relation is transcendental in  $y$ , it must be solved either graphically or numerically. Figure 10 plots three curves: one curve is that for terminal velocity as a function of altitude, and two other curves for the cases in which  $A_0=17.6$  km,  $V_0=330$  m/s, and  $\theta=18^\circ$ , and in which  $A_0=13.8$  km,  $V_0=330$  m/s, and  $\theta=10^\circ$ . The first case corresponds to the earlier free-fall problem, where the object falls from 16 km above Denver to the altitude of Denver, and the second case corresponds to the parameters of the 11 January 1998 fireball at Kiowa, Colorado.

In the first case, the curves intersect at an altitude of 10.7 km and a vertical velocity component of 382 m/s, while in the second case the curves intersect at an altitude of 8.4 km and a vertical velocity component of 330 m/s. Since we know, from above, that for free-fall, the time is:

$$t = \frac{V - V_0 \sin \theta}{g}$$

The free-fall time to from POR to the intersections of the two curves are, respectively, 28.6 sec and 27.8 sec. The rest of the time-of-fall can be determined as follows:

$$\frac{dy}{dt} = \sqrt{\frac{g e^{\beta y}}{k}} = \sqrt{\frac{g}{k}} e^{\frac{\beta y}{2}}$$

$$\frac{dt}{dy} = \sqrt{\frac{k}{g}} e^{-\frac{\beta y}{2}}$$

$$\int_0^T dt = \sqrt{\frac{k}{g}} \int_{y_1}^{y_2} e^{-\frac{\beta y}{2}} dy$$

$$T_{\text{term}} = \frac{-2}{\beta} \sqrt{\frac{k}{g}} e^{-\frac{\beta y}{2}} \Big|_{y_1}^{y_2} = \frac{-2}{\beta} \sqrt{\frac{k}{g}} * \left( e^{-\frac{\beta y_2}{2}} - e^{-\frac{\beta y_1}{2}} \right)$$

**Problem #11: What is the time to fall from a point 16 km above Denver to the surface at Denver?**

a) Assume that Denver is 1.6 km above sea level, and that a meteoroid POR is 16 km (10 mi) above Denver, at an altitude of 17.6 km above sea level. Assume the ground is 1.6 km (1 mi) above sea level. Calculate the time-to-fall to Earth's surface for  $V_0=330$  m/s. Compare to fall time for no atmospheric effects.

b) For the 11 Jan 1998 Kiowa, Colorado event, assume that the POR is 12.2 km (7.5 mi) above Kiowa, at an altitude of 13.8 km above sea level. Assume the ground is 1.6 km (1 mi) above sea level. Calculate the time-to-fall to the Earth's surface for  $V_0=330$  m/s. Compare to fall time for no atmospheric effects.

Solution: a) The free-fall portion of the flight lasts 28.6 sec, as described above. For the terminal-velocity portion of the flight,  $k = 2.74 \cdot 10^{-4} \text{ m}^{-1}$ ,  $\beta = 1/7,536 \text{ m}^{-1}$ ,  $y_2 = 1.07 \cdot 10^4 \text{ m}$ ,  $y_1 = 1.6 \cdot 10^3 \text{ m}$ , and  $g = 9.8 \text{ m/s}^2$ , so the terminal velocity time-to-fall equals:

$$T_{\text{term}} = -2 \times 7,536 \sqrt{\frac{2.74 \cdot 10^{-4}}{9.8}} * \left( e^{-\frac{1.07 \cdot 10^4}{2 \times 7,536}} - e^{-\frac{1.6 \cdot 10^3}{2 \times 7,536}} \right) = -79.7 (0.492 - 0.899) = 32.4 \text{ sec}$$

which, when added to the free-fall flight time of 28.6 sec, equals a total flight time of 61 sec, about 27% longer than the 48-sec fall time derived without regard for atmospheric drag.

b) For the case of the January 11, 1998 Kiowa fireball, the value of  $y_2$  is  $8.4 \cdot 10^3 \text{ m}$  (see intersection of curves on Figure 10), and the value of  $T_{\text{term}}$  is 26 sec, which adds to the 28 sec free-fall time to make a total fall time of 54 sec. This is 22% longer than the 44-sec fall time derived without regard for atmospheric drag.

This concludes the first part of the shallow-entry-angle analysis. The vertical flight profile is defined, and the fall time is bounded. The next part of the problem is to determine the horizontal movement of the meteoroid during the post-POR flight phase.

Unlike the vertical component of motion after the POR, which first increases to a maximum terminal velocity and then gradually decelerates to a terminal velocity of about 190 m/s near the earth's surface, there is no lower limit to the size of the horizontal component of motion, and the horizontal component decreases continually as the meteoroid falls toward the earth's surface. Thus, the object's path will become increasingly steep in the terminal phase of flight, as the

downward rate of travel approaches 190 m/s but the horizontal rate of progress gradually drops toward zero. The following analysis deals with the horizontal rate of slowing during the post-POR flight phase.

For objects moving at less than the speed of sound (330 m/s), the retarding force of the atmosphere is approximately proportional to the square of the velocity. I will use this force relationship as an approximation of the force exerted by the atmosphere on a meteoroid's terminal motion. (All variables refer to horizontal components of meteoroid motion; vertical motion is at terminal velocity):

$$F = ma = m \frac{dV_h}{dt} = -k\gamma m V_h^2$$

where k is the drag coefficient at sea level, and  $\gamma$  is the ratio  $(\rho/\rho_0)=e^{-\beta y}$ , which integrates:

$$\int \frac{dV_h}{V_h^2} = -k\gamma \int dt$$

to yield:

$$-\frac{1}{V_h} = -k\gamma t + C$$

which can be rearranged to yield:

$$V_h = \frac{1}{k\gamma t - C}$$

For  $t = 0$ ,  $V_h = V_0 = V_i \cos\theta$ , so  $C = -1/V_0$ , and the equation becomes

$$V_h = \frac{V_0}{V_0 k\gamma t + 1}$$

(The value of k for a blunt, 5-cm diameter object is about  $2.74 \cdot 10^{-4} \text{ m}^{-1}$ .) Since  $V = dx/dt$ :

$$\int dx = V_0 \int \frac{dt}{V_0 k\gamma t + 1}$$

$$D_x = \frac{\ln(V_0 k\gamma t + 1)}{k\gamma}$$

and, as a non-sequitur sidelight, t varies with x as:

$$t = \frac{e^{k\gamma x} - 1}{V_0 k\gamma}$$

So the equation for  $D_x$  at any given altitude,  $y$ , is:

$$D_x = \frac{\ln \left( (V_i \cos \theta k \gamma t) + 1 \right)}{k \gamma} = \frac{\ln \left( (V_i \cos \theta k e^{-\beta y} t) + 1 \right)}{k e^{-\beta y}}$$

#### 4.4 Application of numerical analysis for determination of $D_x$

##### **Problem #12: Putting it All Together: Example calculations of $D_x$ for some shallow entry-angle events:**

a) Continue the previous Problems (10 and 11) by determining  $D_x$  for the hypothetical case

$V_0=330$  m/s,  $\theta_0 = 18^\circ$ , the meteoroid POR is 16 km (10 mi) above Denver, at an altitude of 17.6 km above sea level. Assume the ground is 1.6 km (1 mi) above sea level. How does this value compare with the solution of Problem 9 that ignores atmospheric effects? What is the descent angle of the objects at the point where they hit the ground? Re-calculate  $D_x$  for the case in which  $V_0=165$  m/s.

b) For the 11 Jan 1998 Kiowa, Colorado event, assume that  $V_0=330$  m/s,  $\theta_0 = 10^\circ$ , the POR is 12.2 km (7.5 mi) above Kiowa, at an altitude of 13.8 km above sea level. Assume the ground is 1.6 km (1 mi) above sea level. How does this value compare with the solution of Problem 11 that ignores atmospheric effects? What is the descent angle of the objects at the point where they hit the ground? Re-calculate  $D_x$  for the case in which  $V_0=165$  m/s. Use the two values of  $D_x$  to define the two ends of the probable strewnfield relative to the POR.

##### **Step-by-step solution:**

a) **Step 1:** Draw the equivalent of Figure 11, with two curves: terminal velocity as a function of altitude,  $y$ :

$$V_{\text{terminal}} = \sqrt{\frac{g e^{\beta y}}{k}}$$

and the free-fall velocity of the meteoroid (vertical component only) as a function of altitude:

$$V_{y, \text{free-fall}} = \sqrt{2g(A_0 - y) + V_0^2 \sin^2 \theta}$$

Be sure to use values for both  $y$  and  $A_0$  that are relative to sea level, not to the earth's surface (this is important for Colorado fireballs).

The altitude,  $y$ , at which the free-fall vertical velocity component equals the terminal velocity is given by the value of  $y$  that satisfies the relation:

$$\sqrt{2g(A_0 - y) + V_0^2 \sin^2 \theta} = \sqrt{\frac{g e^{\beta y}}{k}}$$

and this is the point where the two curves intersect. Referring to Figure 10, for part (a) of this problem, the two curves intersect at:

$$y = 10.7 \text{ km}, V_y = 382 \text{ m/s}$$

This is the place and the downward velocity at which free-fall flight converts to terminal velocity flight. A traveller inside the meteoroid would go from a weightless condition to a weight of 1 g at this point.

**Step 2:** Draw up a table, and determine time-to-fall through altitude increments, as follows:

Table IV. How to start the  $D_x$  analysis for accommodation of atmospheric drag effects.

y (km, MSL)	$\rho/\rho_0=\gamma$	Time-to-fall (sec)	$V_x$ @ upper altitude (m/s)	$D_x$ (m)	$V_x$ @ lower altitude (m/s)
17.6-15	0.115	14.9			
15-10.7	0.182	13.6			
10.7-10	0.253	1.9			
10-5	0.370	16.1			
5-1.6	0.645	14.5			
Total fall dist		Total fall time		Total $D_x$	
16 km		61.0 sec			

The rule for constructing the first column is to break the total height of the fall into 5-km increments, nominally 0-5, 5-10, 10-15, 15-20, etc. But for the lowest increment, set the lowest altitude to the altitude at which the fall came to rest (about 1.6 km MSL for the Colorado high plains). Also, create a break for the altitude at which free-fall flight converts to terminal-velocity flight (10.7 km MSL, in this case). Finally, convert the highest altitude to the height of the POR relative to sea level (17.6 km MSL, in this case).

For the second column, calculate the average density relative to sea level for each row by taking the arithmetic average of the high and low altitude for each row, and then inserting the average altitude into the relation:

$$\frac{\rho}{\rho_0} = e^{-\beta y}$$

where  $y$  is in kilometers and  $\beta = (1/7.536) \text{ km}^{-1}$ . For example, the average of 10-to-5 km is 7.5 km. Inserting this into the equation gives a density ratio of  $e^{-(7.5/7.536)} = 0.370$ .

In the third column, the time-to-fall is calculated using the free-fall equation down to the intersection point (in this case, the first two rows of the table):

$$T_{\text{free fall}} = \frac{-V_0 \sin\theta + \sqrt{V_0^2 \sin^2\theta + 2gA_0}}{g}$$

Treat all physical quantities as positive. For this example, the first row is calculated for  $A_0 = 17,600 - 15,000 \text{ m} = 2,600 \text{ m}$ , which yields 14.9 sec fall time for the first row. For the second row,  $A_0 = 17,600 - 10,700 \text{ m} = 6,900 \text{ m}$ , which yields 28.5 sec fall time. But this fall time

includes the 14.9 sec to fall through the first row. So the entry for the second row is 28.5 - 14.9 sec = 13.6 sec. Continue this process for all free-fall rows.

For the terminal-velocity rows, the time-to-fall is calculated from:

$$T_{\text{terminal fall}} = \frac{-2}{\beta} \sqrt{\frac{k}{g}} \cdot \left( e^{\frac{-\beta y_2}{2}} - e^{\frac{-\beta y_1}{2}} \right)$$

where  $y_2$  and  $y_1$  are the altitudes of the upper and lower edges of the row, respectively. The values of  $k$  and  $\beta$  are  $2.74 \cdot 10^{-4} \text{ m}^{-1}$  and  $1/7,536 \text{ m}^{-1}$ , respectively. Calculate the terminal velocity fall-time for each row, down to the ground.

**Step 3:** Determine the horizontal displacement for each altitude increment.

The fourth and sixth columns are filled in first, using the equation:

$$V_h = \frac{V_0}{V_0 k \gamma t + 1}$$

where  $V_0$  is the horizontal component of the motion at the *upper edge* of each row. In this example, the calculation goes as follows:  $V_i \cos \theta = (330 \text{ m/s}) \cdot \cos(18^\circ) = 314 \text{ m/s}$ . This is the value for the first row, fourth column. The value for the first row, sixth column, is:

$$V = \frac{314}{(314 \cdot 2.74 \cdot 10^{-4} \cdot 0.115 \cdot 14.9) + 1} = 274 \text{ m/s}$$

This value of  $V$  is also the *initial value for the fourth column in the next row*. The sixth column in the next row is calculated as above, this time using the values of average density and time-to-fall for that row:

$$V = \frac{274}{(274 \cdot 2.74 \cdot 10^{-4} \cdot 0.182 \cdot 13.6) + 1} = 231 \text{ m/s}$$

which is the value for the second row, sixth column, and also for the third row, fourth column. Fill in the entire table for the fourth and sixth columns:

Table V. Continuation of development of Table IV.

y (km, MSL)	$\rho/\rho_0=\gamma$	Time-to-fall (sec)	$V_x$ @ upper altitude (m/s)	$D_x$ (m)	$V_x$ @ lower altitude (m/s)
17.6-15	0.115	14.9	314		274
15-10.7	0.182	13.6	274		231
10.7-10	0.253	1.9	231		224
10-5	0.370	16.1	224		164
5-1.6	0.645	14.5	164		115
Total fall dist		Total fall time		Total $D_x$	
16 km		61.0 sec			

Now it only remains to fill in the column for horizontal displacement values as a function of altitude. For each row interval, use the equation:

$$D_x = \frac{\ln(V_0 k \gamma t + 1)}{k \gamma}$$

where  $V_0$  is the value in the *fourth column* for each row interval. For example, in the first row,  $V_0$  is 314 m/s, and  $\gamma$  is 0.115. Thus  $D_x$  for the first row is:

$$D_x = \frac{\ln((314 \cdot 2.74 \cdot 10^{-4} \cdot 0.115 \cdot 14.9) + 1)}{2.74 \cdot 10^{-4} \cdot 0.115} = 4360 \text{ meters}$$

Continuing this process, and using the corresponding  $V_0$  and density values for each row, we complete the table:

Table VI. Example fireball, POR=16 km above Denver,  $V_0=330$  m/s,  $\theta=18^\circ$ .

y (km, MSL)	$\rho/\rho_0=\gamma$	Time-to-fall (sec)	$V_x$ @ upper altitude (m/s)	$D_x$ (m)	$V_x$ @ lower altitude (m/s)
17.6-15	0.115	14.9	314	4360	274
15-10.7	0.182	13.6	274	3420	231
10.7-10	0.253	1.9	231	432	224
10-5	0.370	16.1	224	3070	164
5-1.6	0.645	14.5	164	1990	115
Total fall dist		Total fall time		Total $D_x$	
16 km		61.0 sec		13.3 km	

Note that the fall times that have been calculated are exact, neglecting the transition time from free-fall flight to terminal velocity flight. The determination of horizontal displacement is an approximation, but can be made arbitrarily accurate by using smaller altitude increments.

In this case, the total horizontal displacement is about 11% less than the non-atmospheric estimate.

For this example, we were also asked to calculate the total  $D_x$  value for a initial velocity 165 m/s, with the same altitude and initial descent angle. With reference to Figure 11, the new intersection between free-fall and terminal flight now becomes 10.4 km, and the table is:

Table VII. Example fireball, POR=16 km above Denver,  $V_0=165$  m/s,  $\theta=18^\circ$ .

y (km, MSL)	$\rho/\rho_0=\gamma$	Time-to-fall (sec)	$V_x$ @ upper altitude (m/s)	$D_x$ (m)	$V_x$ @ lower altitude (m/s)
17.6-15	0.115	18.4	157	2760	144
15-10.4	0.185	15.1	144	2060	130
10.4-10	0.258	1.1	130	142	129
10-5	0.370	16.1	129	1890	107
5-1.6	0.645	14.5	107	1370	84
Total fall dist		Total fall time		Total $D_x$	
16 km		65.2 sec		8.2 km	

The result of these calculations is that the strewnfield may be estimated to be displaced horizontally between 8.2 km and 13.3 km from the POR. Thus, the strewnfield may be estimated to have a total length of about 5.1 km (3.2 mi).

Assuming a final vertical velocity component of 190 m/s, the vertical descent angle when the meteorite hits the ground for this example would be between  $59^\circ$  (for  $V_0=330$  m/s) to as much as  $66^\circ$  (for  $V_0=163$  m/s).

#### 4.5 Calculation of $D_x$ for the 11 Jan 1998 Kiowa fireball

The two following tables were constructed for this event, assuming the conditions of Problem 12:

Table VIII. 11 January 1998 Kiowa fireball, POR=12.2 km above Denver,  $V_0 = 330$  m/s,  $\theta=10^\circ$ .

y (km, MSL)	$\rho/\rho_0=\gamma$	Time-to-fall (sec)	$V_x$ @ upper altitude (m/s)	$D_x$ (m)	$V_x$ @ lower altitude (m/s)
13.8-10	0.206	22.6	325	6140	230
10-8.4	0.295	5.3	230	1160	209
8.4-5	0.411	11.6	209	2140	164
5-1.6	0.645	14.5	164	1990	115
Total fall dist		Total fall time		Total $D_x$	
12.2 km		54 sec		11.4 km	

Table IX. 11 January 1998 Kiowa fireball, POR=12.2 km above Denver,  $V_0 = 165$  m/s,  $\theta=10^\circ$ .

y (km, MSL)	$\rho/\rho_0=\gamma$	Time-to-fall (sec)	$V_x$ @ upper altitude (m/s)	$D_x$ (m)	$V_x$ @ lower altitude (m/s)
13.8-10.0	0.206	25.1	163	3680	132
10.0-8.3	0.295	5.6	132	718	125
8.3-5.0	0.411	11.2	125	1300	108
5.0-1.6	0.645	14.5	108	1380	85
Total fall dist		Total fall time		Total $D_x$	
12.2 km		56.4 sec		7.1 km	

These results indicate that the most likely horizontal displacement for the 11 January 1998 Kiowa fireball strewnfield is an ellipse that runs between 7.1 km to 11.4 km (4.4 mi to 7.1 mi) from the POR. The length of the strewnfield is probably about 4.3 km (2.7 mi).

Assuming that the vertical velocity of the meteorites was about 190 m/s when they hit the ground, the final vertical descent angle for these pieces would have been between about  $59^\circ$  (for  $V_0 = 330$  m/s) to  $66^\circ$  (for  $V_0 = 163$  m/s). It is a coincidence that these final vertical descent angles are the same as for part (a) of this problem.

#### 4.6 Guidelines for calculation of $D_x$ for shallow meteoroid angles

There are many sources of uncertainty in the calculation of  $D_x$  for shallow-angle events, and some of them are significant. Variables that are not usually precisely known are the descent angle,  $\theta$ , and the altitude of the point-of-retardation. But, with collection of a large number of witness accounts, it should at least be possible to obtain reasonably good estimates for these two variables.

Precise values of the initial velocity,  $V_0$ , and for the coefficient of the retarding horizontal force,  $k$ , for each of the falling objects are not normally measurable, and cannot be known with precision from first principles (although the initial velocity can be inferred if a camera system records the event). Thus, we are presented with a problem in which we may have a reasonably good mathematical model for the fall, but we do not have measured values for most of the significant parameters in the model.

Is it possible to calculate  $D_x$  accurately? It is certainly not possible to calculate a single value of  $D_x$  for any given fall, since a fall will normally consist of many separate objects, and will occupy a strewnfield. It is possible to at least estimate  $D_x$  using the procedure outlined above. In this procedure, use the best possible estimates for the altitude of the POR and for the descent angle. Then, use the model to calculate the values of  $D_x$  for two values of  $V_0$ : 330 m/s and 165 m/s.

Measuring horizontally from the coordinates of the POR, mark these two values of  $D_x$  along the direction of the fireball's flight track. If crosswinds are not known, estimate perhaps half the difference between these two values of  $D_x$  as the width of the strewnfield. Then, draw an ellipse between these four points ( $D_x$  minimum,  $D_x$  maximum, and the two points that are at right angles to the  $D_x$  points and that are on a line half way between them).

Figure 10. Intersection of free-fall and terminal velocity curves.

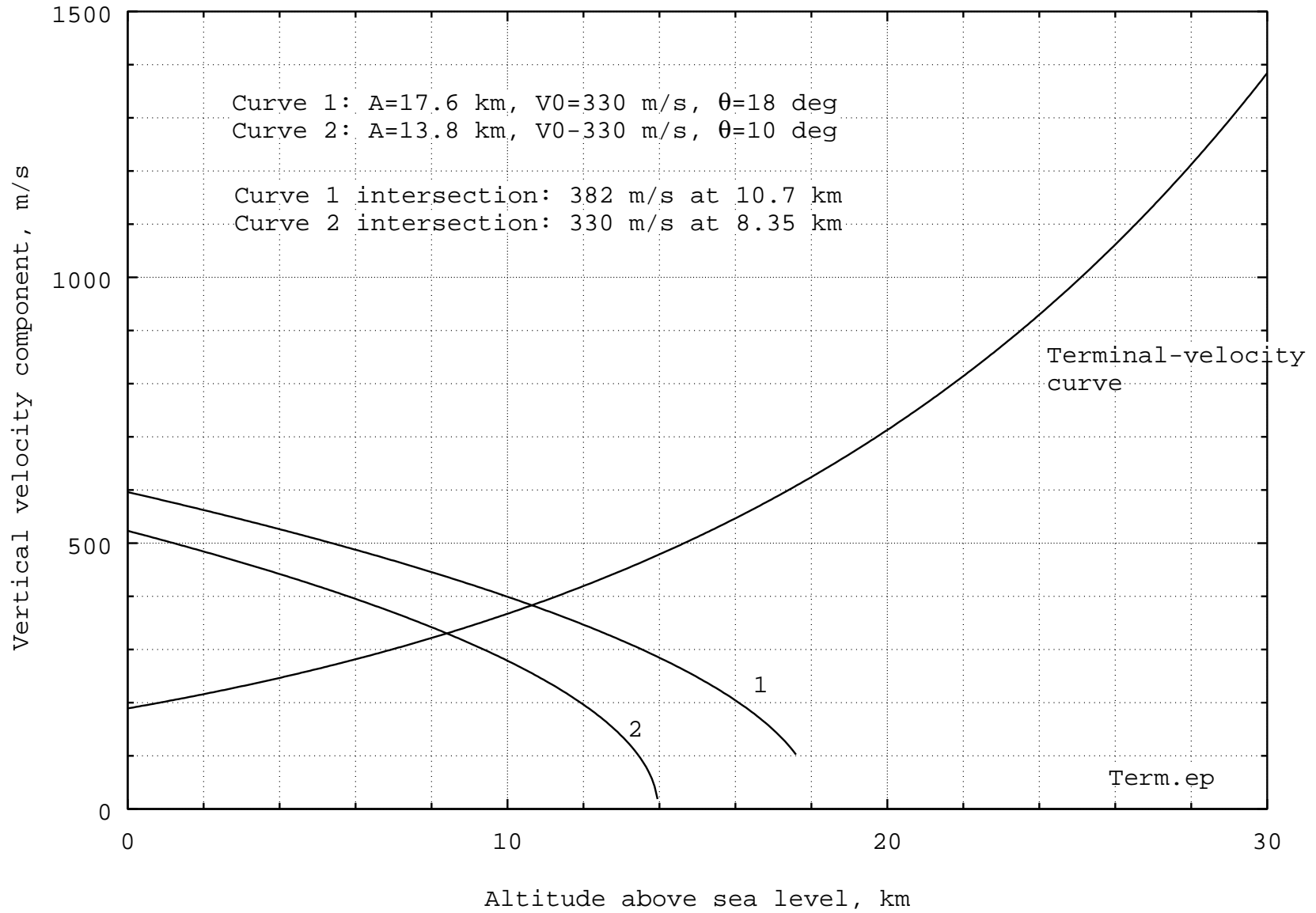
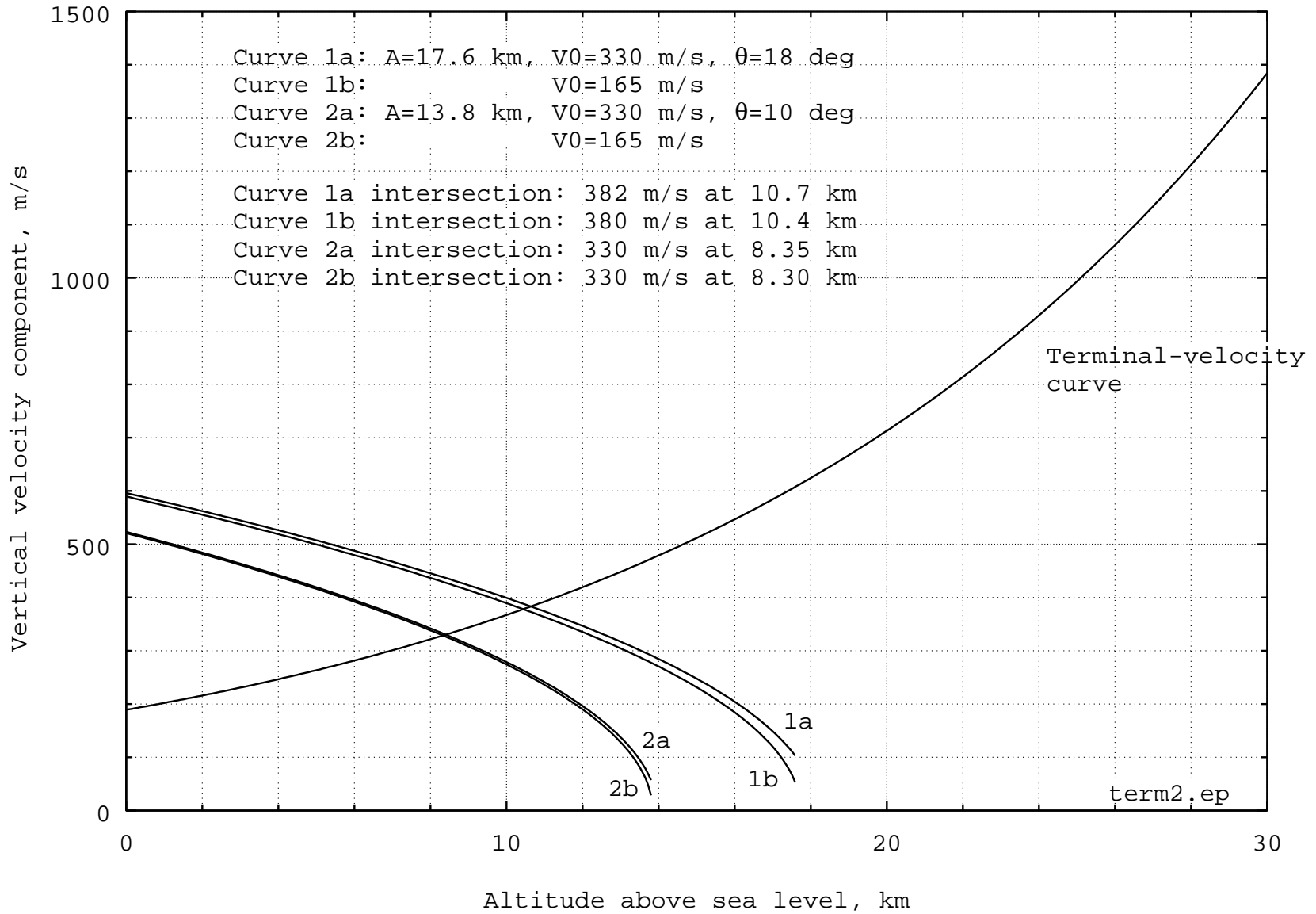


Figure 11. Intersection of free-fall and terminal curves for Problem 12.



The process for determining  $D_x$  as described in the construction of the tables is *numerical integration*. The process can be made more accurate by breaking the fall distance into smaller increments (in effect, adding rows to the table). While this would be cumbersome to do by hand, it would be easy to implement as a computer program. The author has written such a program.

This is probably the best method<sup>10</sup> that is available to researchers who are searching for the strewnfield of a fall--it is a tool that allows the search for the fall to be conducted in an area that has the highest probability of yielding meteoroids from a fireball event.

## BIBLIOGRAPHY

J. Kelly Beatty and Andrew Chaikin, eds., *The New Solar System*, Third Ed., Sky Publishing Corporation, 1990.

Craig Covault, USAF Missile warning satellites providing 90-sec. scud attack alert, *Aviation Week and Space Technology*, January 21, 1991, p. 60-61.

Editors of Defense Electronics, Defense support program, in *The C3I Handbook*, Third Edition, EW Communications, Inc., 1988.

Jerry B. Marion, *Classical Dynamics of Particles and Systems*, 2nd ed., Academic Press, 1970.

O. Richard Norton, *Rocks from Space*, second ed., Mountain Press Publishing, 1998.

David A. Rothery, *Satellites of the Outer Planets: Worlds in Their Own Right*, Clarendon Press, 1992.

Howard Seifert, ed., *Space Technology*, Chapter 13, *The Possibility of a Safe Landing*, Alfred J. Eggers, Jr., Wiley & Sons, Inc., 1959.

---

<sup>10</sup>The author has found no method in print for locating strewnfields relative to the POR; this is his own model, but it appears to provide results that accord with known strewnfield locations. Refinements of this model are anticipated in the future.

## REFERENCES

1. Allen, H.J., and A.J. Eggers, Jr., "A Study of the Motion and Aerodynamic Heating of Missiles Entering the Earth's Atmosphere at High Supersonic Speeds," NACA TN 4047; October 1957.
2. Eggers, A.J., Jr., H.J. Allen, and S.E. Niece, "A Comparative Analysis of the Performance of Long-Range Hypervelocity Vehicles," NACA TN 4046; October 1957.
3. Eggers, A.J., Jr., C.F. Hansen, and B.E. Cunningham, "Stagnation-Point Heat Transfer to Blunt Shapes in Hypersonic Flight, Including Effects of Yaw," NACA TN 4229; April 1958.
- 3a. Editors of Defense Electronics, Defense support program, *in* The C3I Handbook, Third Edition, EW Communications, Inc., Palo Alto, p. 51-52; 1988
- 3b. Covault, Craig, USAF Missile warning satellites providing 90-sec. Scud attack alert, *Aviation Week and Space Technology*, January 21, 1991, p. 60-61.